

February 10th, 2017

Dear Editor,

At first, we would like to thank you for serving as the editor for our work.

We would like to inform you that we have revised the manuscript significantly based on the comments by three reviewers. We believe that the comments have certainly helped improve the quality of our analysis and interpretations. We have shortened various sections, and also inserted new sections in order to incorporate reviewers' comments and hence strengthen our analysis and discussion. Sections on ratios of PM fractions, BC/CO ratios, and influence of meteorology on pollution concentrations have been inserted whereas section on model based aerosol composition has been taken out following the reviewer's suggestions. Moreover, new figures have also been included to explain the findings from our work. Finally, the abstract and conclusion section have been rewritten to reflect the updated findings.

Sincerely Yours,

Dipesh Rupakheti and Prof. Shichang Kang, on behalf of all coauthors

Pre-monsoon air quality over Lumbini, a world heritage site along the Himalayan foothills

by D. Rupakheti et al., 2016 (ACPD)

We would like to thank the reviewers for their constructive comments and suggestions. Please find the [reviewer's comments in black and our replies in blue](#). The [changes in the revised manuscript are colored in red](#).

REVIEWER-1

In this paper, authors present measured ambient PM, BC, CO and O₃ concentrations in Lumbini during an intensive measurement campaign from April-June 2013. They also conducted a regional WRF-STEM modeling to simulate the meteorology and air pollutant concentrations, as well as to examine the aerosol chemical composition. The authors conclude that there is high pollution in Lumbini and that a network of long-term air quality monitoring stations is needed in the greater Lumbini region. I agree with the authors that it is important to collect observational data in this area and the set of observations presented in the paper is extremely useful for understanding the magnitude of the air pollution problem and the potential sources. However, the language is very vague and the scientific discussion is limited. I find that the improvements are essential before the manuscript can be published in ACP. I list some of the concerns below.

We would like to thank the reviewer for considering the work we have conducted over Lumbini important. We have tried our best to incorporate reviewer's comments and suggestions in the following sections.

I am unsure if what we are most interested in is the comparison of Lumbini measurement with those of other cities. For example, they state that "BC observed at Lumbini was higher by a factor of ~6 and ~4.5 compared to that at Mt. Abu, India and near the base of the Mt. Everest, Nepal, respectively (1.323-326)" but how do we know what to make of these comparisons. What do we learn from these comparisons? To me, it is logical that Lumbini has higher BC

concentrations compared to those remote places. Similarly, I do not find interesting that the ozone concentrations were higher at Lumbini than in the Mt. Everest (l. 332). I would rather be more interested to know how the monthly concentrations change and when the highest and lowest concentration levels were and if there was any difference in the three months or over time among the species.

By comparing with other stations, we intend to show the status of air quality in Lumbini. We have rewritten the section in order to make it more scientific. Moreover, we calculated the monthly concentration change as suggested by the reviewer (see the [Figure S5](#)) and added a description in the text ([Section 3.2.1](#)). Changes are made in lines 378-400 (lines 394-400 for monthly variation) of the revised manuscript.

Regarding the ozone concentration at Lumbini, we have mentioned that the ozone at Lumbini was (l. 332) found to be lower than at the Mt. Everest region, and have provided the possible reasons for that phenomenon. Please see the [Section 3.2.2](#) in the revised manuscript.

Changes are made in lines 388-393 in the revised manuscript.

Also, examining the period when the model is able to reproduce observations and contrasting that to the times when the model fails would be a good way to make use of both measurements and the model. Such assessment should also provide a good basis for what needs to be improved in the model. I find the argument that the authors put forward on l. 261-262 that the “[D]iscrepancy on model results might have occurred due to various factors inherently uncertain in a weather model” to be hand-waving and not really helpful. With this data set, they should be able to understand the discrepancy between model and the observations a little better.

We thank the reviewer for this suggestion. As per the advice of other reviewers as well, we now have revised the manuscript to focus more on observation data. The model is used to explain only anthropogenic emission source regions (excluding open burning) using tagged CO tracers. Aerosol modeling studies will be a scope for future paper as model needs improvement (stated in [Section 3.2.2](#)).

The manuscript does describe when the model is able to perform well for CO concentration versus times when the predictions are poor (section 3.2.2 and section 3.3.1).

Why is PM1 concentration not discussed in the study (l. 282-283)? If it is discussed elsewhere, please mention it. If there was a problem with the data, then I think this should not be included in this manuscript at all. If there was no problem with the data, I think that can provide an additional insight into the measurements and is worth exploring more than just the average concentrations mentioned in l. 281.

There was no problem with the PM1 data as the instrument provided the concentration of PM10, PM2.5 and PM1 simultaneously. We have included the discussion on PM1 on the revised MS. Reviewer-2 also raised the similar concern. Please see the reply to Reviewer-2 as well on this matter. New additions are shown in lines 273-277, lines 285-296 of the revised manuscript.

I am quite confused about WRF-STEM model simulations. Authors state: “A comparison of model calculated average concentration along with the minimum and maximum concentrations of various pollutants (with observation) is shown in Table 3 (l.340-342).” However, right after this sentence, they write that “[T]he model based concentrations used here are instantaneous values for every third hour of the day (l. 342-343).” Can authors clarify which one that is and if the latter, why did they use the instantaneous values?

Thank you for pointing out this confusion. We mean to say that the model based concentrations were obtained at every third hour unlike the monitoring values. We also would like to make it clear that the modeling values reported in the whole manuscript is every third hour instantaneous value. This is corrected in the revised manuscript.

There are many places where authors state in a very qualitative manner, which obviously is not helpful for the reader to understand the issues being discussed. I list some of the sentences here:

We would, again, like to thank the reviewer for pointing this out. We have tried our best to explain and rephrase the sentences to make it scientific.

1. 1.298-299 “BC to CO ratio in Lumbini was found to be different from that observed at other urban and rural sites and those affected by forest fire/biomass burning.” What was the ratio observed at Lumbini and other places? What can we infer from this? What is the criterion for “different”?
2. 1. 299-302 “a suburban site, Pantnagar, in IGP also observed similar BC to CO ratio.” What value is considered “similar” and how is that determined? What do we learn from this?

Here we respond to comment #1 and #2 together. By the sentences as mentioned in l. 298-302, we intend to explain that the ratio of BC to CO observed at Lumbini were different from the ratio obtained over other sites (from literatures) except Pantnagar and Maldives. Reviewer-2 also raised the similar concern. Please see the reply to Reviewer-2 on this matter as well. Changes are shown in lines 324-339 of the revised manuscript.

3. 1. 318-321 “PM_{2.5} concentration in Lumbini have been found to be lower than the megacity like Delhi and north-western IGP regions due to higher level of emissions over those regions.” How did they come up with this conclusion? I do not see any comparison of emissions, especially at the sector level. Also, I understood that changing emissions in Lumbini and surrounding regions did not lead to a large concentration difference in the model when they conducted a sensitivity analysis (l. 474-488). Doesn’t this conflict with what is argued here?
4. 1. 321-323 “BC concentrations observed in Lumbini during pre-monsoon season was lower than the urban Asian cities like Kathmandu and Delhi, slightly higher than in Kanpur but high compared to the remote locations in the region.” Are the authors comparing the measurements during the same period between cities? What does “slightly higher” and “high” mean? What is the definition of these? More importantly, what do we learn from this?

Here we respond to comments #3 and #4 together. Unfortunately, we have not conducted any comparison on emission at sector level. We rather conducted comparison on concentrations. We compared the pre-monsoon seasonal average concentrations of BC, PM_{2.5}, CO and O₃ obtained at Lumbini with other nearby sites (as mentioned in Table 2). The words like “slightly higher”

and “high” have been removed and the whole paragraph have been rephrased, as already provided in the response to the reviewer’s earlier question. Please see lines 382-389 for the changes in the revised manuscript.

5. 1. 355-359 “STEM model performance can be significantly improved via better constraining anthropogenic emissions inventory, emissions of open biomass burning and improvements in meteorological output from WRF amongst many other uncertainties inherent in regional chemical transport model.” How did they get to this conclusion?

Modeling scope for this current paper has been reduced as per reviewer advice and the associated sentences have been revised throughout the manuscript. However, for the above sentence, pollutant concentration is a function of meteorology (including transport), emissions, and physical and chemical transformation. Many of these processes are parameterized or not accounted in the model. Improvements in any one of these or all of these will lead to improvement in model skills.

6. 1. 526-529 “The curve during the prime cooking time is much close to the biomass curve of published data whereas that during non-cooking time is inclined towards the fossil fuel curve.” How is “much close” determined, as well as “inclined”?

We have rephrased this sentence in the revised manuscript with a new sentence and provided the comparison figure (Figure 14 in revised manuscript) with published data (to remove the confusion) on biomass and fossil fuel burning as below:

The curve obtained for the prime cooking time is closer towards the published curve on biomass burning whereas that obtained during the non-cooking time is closer towards the published fossil fuel curve.

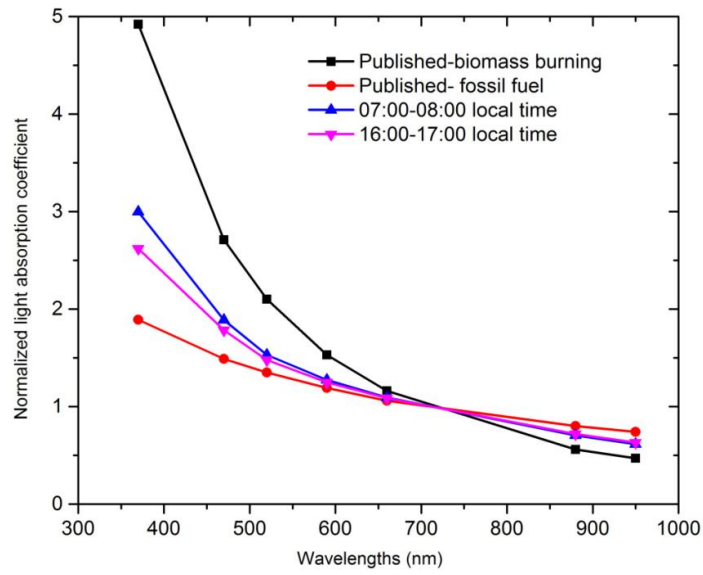


Figure 14: Comparison of normalized spectral light absorption coefficients obtained during the prime cooking (07:00-08:00 local time) and non cooking time (16:00-17:00 LT) at Lumbini with published data from Kirchstetter et al. (2004).

For the two events when authors found and elevated BC and CO concentrations, what were the PM and O₃ levels? Did they find an elevated PM on any other days? Did they find an elevated potassium levels during those days? I think that focusing on the analysis of these two events and clearly explaining the details of the regional contribution assessment presented in the manuscript would definitely strengthen the paper. The regional contribution assessment could be also extended by quantifying the monthly differences and also considering other species. This then could be linked to the chemical composition to assess if the regional contribution has anything to do with the chemical composition difference that they can potentially see in different months.

PM concentrations during two events were 267.33 ± 12.51 (PM₁₀), 107.27 ± 9.20 (PM_{2.5}) and 76.75 ± 7.67 (PM₁) $\mu\text{g}/\text{m}^3$ during Event-I (i.e., 7-9th April, 2013) and 297.60 ± 75.48 (PM₁₀), 117.90 ± 34.85 (PM_{2.5}) and 84.42 ± 25.27 (PM₁) $\mu\text{g}/\text{m}^3$ during Event-II (i.e., 3-4th May, 2013). Similarly O₃ concentrations were found to be $53.47 (\pm 2.57)$ and $56.75 (\pm 8.35)$ ppbv during Event-I and Event-II, respectively. The TSP sampling was conducted in coarse resolution (once in 3-6 days) due to which we unfortunately missed the sampling during the events days to evaluate the potassium level during the events.

The chemical composition analysis has been removed from the manuscript as suggested by other reviewers, and it also requires the work beyond the scope of this paper. However, we have added the monthly variation part (in Section 3.3.2) as suggested by the reviewer which reads as:

Regarding the monthly average contribution, the Ganges Valley and Nepal's contribution were almost equal during the month of April (~34% and ~37% respectively) but increased for the Ganges Valley region during the month of May (~44%) in which contribution of Nepal region got reduced (~25%) (Figure S6).

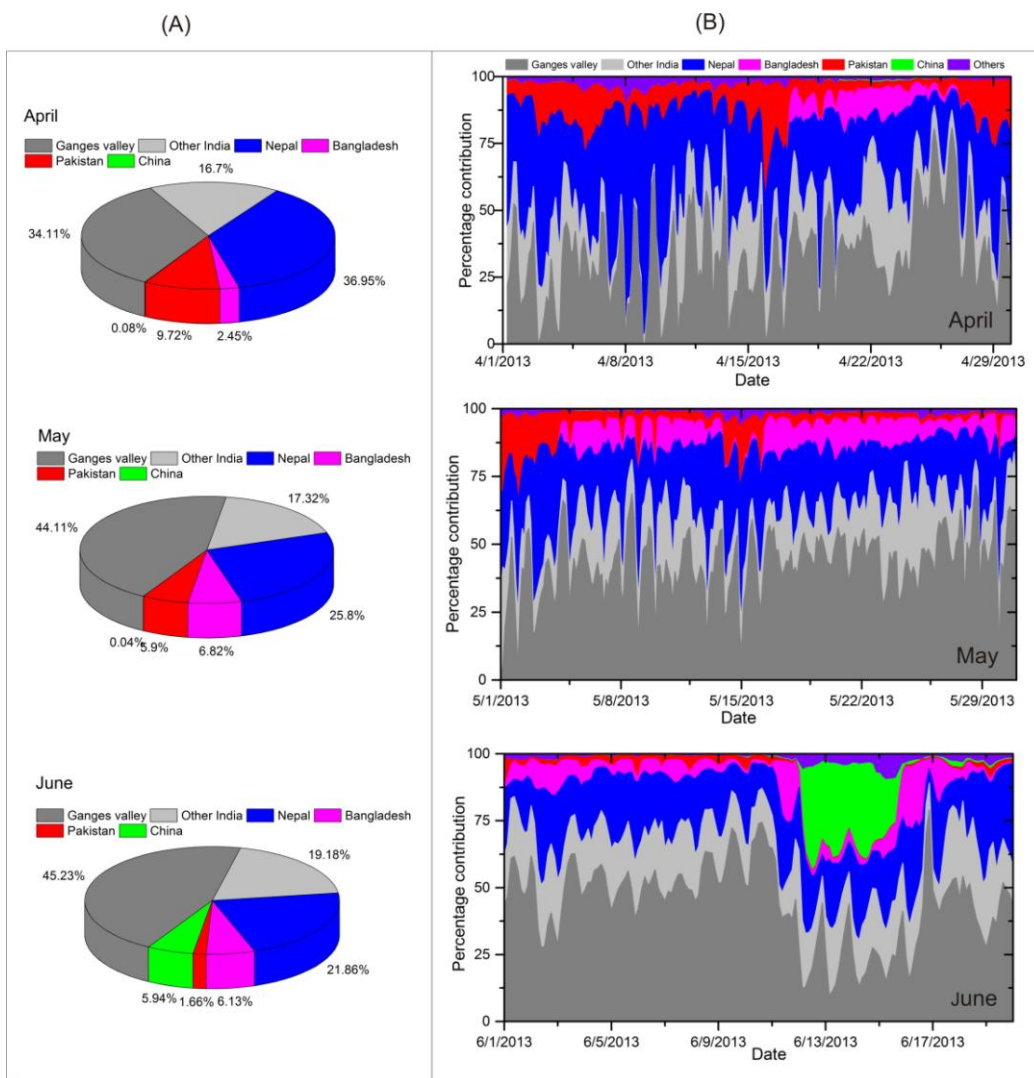


Figure S6: (A) Monthly average model estimated contributions of various source regions to average CO in Lumbini and (B) Time series of region tagged CO tracer during individual months.

Minor comments:

1. rain guage→ rain gauge (l. 239)

Corrected

2. I'm not sure if the authors really meant the way they wrote the sentence: "But, to our expectation, we could not observe any significant influence of forest fires within the specified grid (l. 419-420)." Did the authors really expect that they would not be able to observe influence? Or is this a typo?

We would like to thank the reviewer for pointing this out. At first, we were speculating the influence of the forest fires within the specified grid (local forest fire) for the occurrence of events in Lumbini. Later on, when we analyzed the forest fire over the larger region (as shown in Figure 9 and 10 in the ACPD MS), the influence of regional forest fire over our study site was confirmed.

3. Others region→ other regions (l. 469)

Corrected

References

Kirchstetter, T. W., Novakov, T., and Hobbs, P. V.: Evidence that the spectral dependence of light absorption by aerosols is affected by organic carbon, *J. Geophys. Res.*, 109, D21208, doi:10.1029/2004JD004999, 2004.

REVIEWER-2

General comments

The paper reports for the first time in Lumbini, Nepal, BC, CO, O₃ and PM data from a 3-month experiment in one site. The motivation is to understand air quality in Lumbini, but this objective sounds oversized in regard of the limited duration of the experiment. By the way, no scientific question is set and the methodology presents weak points. Data are new but rather few. No chemical speciation is provided to complete the data of species monitored online. Moreover, those online data could have been further treated: by using ratios (e.g., BC/CO, K/BC, PM₁/PM_{2.5}) and the aethalometer model to take full benefit from the BC spectral dependence. The use of modeling is useful to study the synoptic variability of pollutants, but appears highly questionable to simulate the chemical components, given the poor emission data used. A shorter manuscript, attempting to better understand for instance the source effects of the major emission points affecting Lumbini, using data only, not modeling could be considered.

We have tried our best to address the queries and suggestions raised by the reviewer. Scientific question has been provided in the revised manuscript. We feel sorry that we don't have the chemical speciation in this work which is beyond the scope of this paper. The revised manuscript includes substantial discussion using ratios to understand behavior and sources of pollutants. As the reviewer raise concern on the chemical components provided by the model, we have removed compositional analysis portion from the paper in the revised version.

Specific comments

22 Abstract: Objectives and/or a specific question need to be clearly stated.

We have added the objective of our study in the abstract/introduction section.

The main objective of this work was to understand the level of air pollution, diurnal characteristics and the influence of open biomass burning on air quality in Lumbini.

178 Was any cut-off applied on the BC sampling line, or was it bulk BC?

No specific cut-off was applied on the BC sampling. Hence, the BC concentration reported in the manuscript is total suspended BC (lines 166-167 of the revised manuscript).

282 It is a pity that PM1 was not considered. The variations of the PM1-to-PM2.5 ratio would possibly provide interesting information about source profiles.

We did not discuss the PM1 concentration in the discussion version of the manuscript. It was not intentional. We have included PM1 now. Based on the suggestions from other reviewers (#1 and 3) as well, we have revised the General overview section (3.2.1) as **General overview, PM ratios and influence of meteorology on pollution concentrations** which now includes the ratios PM1-to-PM2.5, PM2.5-to-PM10, BC-to-PM1 and BC-to-PM2.5 and also the influence of meteorology on concentrations of monitored pollutants. Please see the Section 3.2.1 in the revised manuscript.

296 Both BC and CO are from incomplete combustion process but the ratio BC/CO is often specific to the different processes. A plot of the variations of BC/CO in time could be more relevant than BC and CO separately.

414 BC and CO originate from biomass burning as well as from any other fuel and combustion types, as mentioned earlier (line 296). Thus this sentence does not justify the use of BC and CO. Instead, BC/CO could help for source discrimination.

Agree. Regarding the Line 296 (Figure S2), a plot showing the time series of $\Delta BC/\Delta CO$ during the monitoring period has been inserted. In addition, we have also compared the average $\Delta BC/\Delta CO$ ratio observed at Lumbini with other sites (Figure 7) and have included in the main text. The discussions on the new figures have been inserted in the revised version of the manuscript (Section 3.2.1).

Moreover, as suggested by the reviewer, we have replaced the Figure 9 (of ACPD version) with the new figure (Figure 10) provided below where the ratio of $\Delta BC/\Delta CO$ (daily average concentration) has been plotted instead of BC and CO separately.

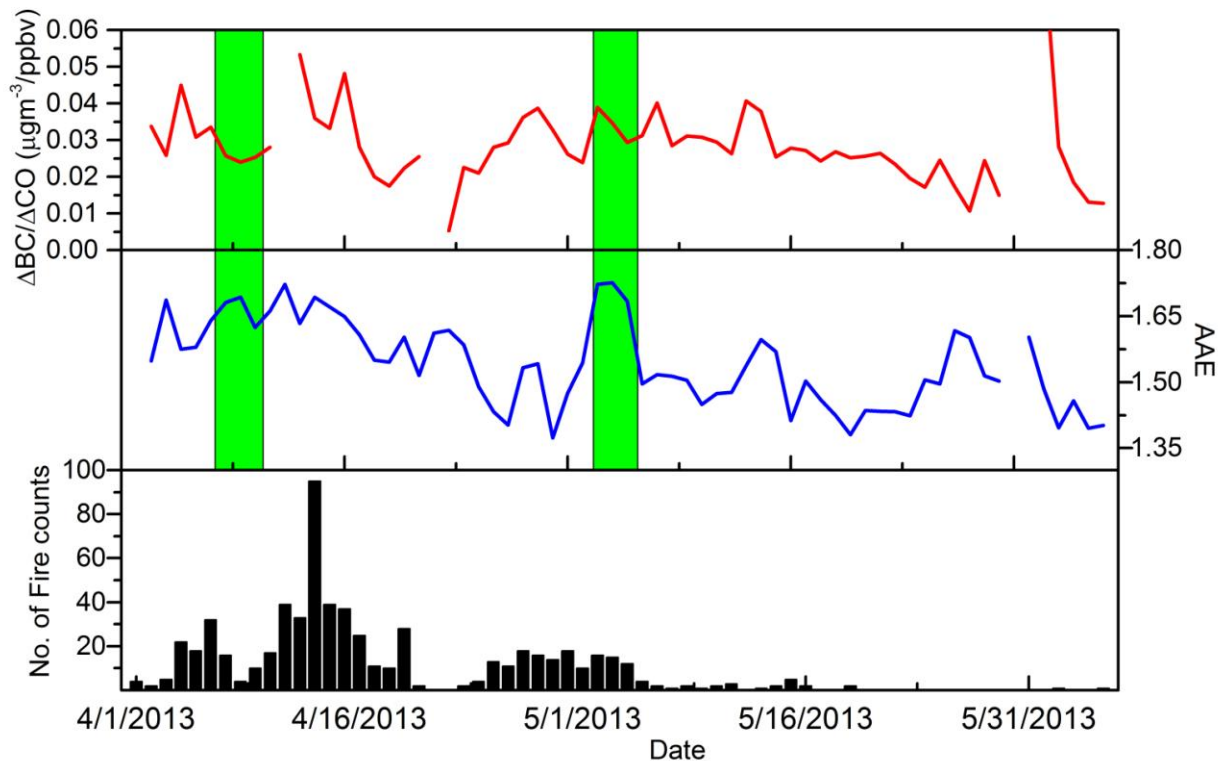


Figure 10. Time series of daily average $\Delta BC/\Delta CO$ ratio and absorption Ångström exponent (AAE) derived from observations, along with fire counts acquired with the MODIS instrument onboard TERRA satellite for a 200×200 km grid centered at Lumbini. Two rectangular green boxes represent time of two episodes with high peaks in CO and BC concentrations as shown in earlier figures.

417 Potassium is a biomass burning tracer when the fine fraction is considered. As it can have other sources, it is rather examined as K/BC.

Agree. In the manuscript, we just want to state that the potassium concentration during the pre-monsoon season is higher in the whole year. In order to examine the K/BC ratio, we don't have (at least) a yearlong BC concentration from Lumbini. Recently, our group identified that the K^+ in Lumbini is mostly from dust (Wan et al., 2016; manuscript under review for ACPD). So, we have rephrased the sentence in [Section 3.3.1](#) which reads as below:

The chemical composition of TSP filter samples collected at Lumbini also showed higher concentration of Levoglucosan, a biomass burning tracer in Lumbini during the pre-monsoon season as compared to other seasons of the year (Wan et al., 2016). Moreover, Wan et al. (2016) also reported that the highest correlation coefficient between K^+ and tracers of dust (Ca^{2+} and Mg^{2+}) indicating that dust is the main source of potassium in Lumbini.

Reference:

Wan, X., Kang, S., Li, Q., Rupakheti, D., Zhang, Q., Guo, J., Chen, P., Tripathee, L., Rupakheti, M., Panday, A.K., Wang, W., Kawamura, K., Gao, S., Wu, G. and Cong, Z.: Organic molecular tracers in the atmospheric aerosols from Lumbini, Nepal, in the northern Indo-Gangetic Plain: Influence of biomass burning, Manuscript under review for ACPD, 2016.

563 Remove PM1

We have discussed the PM1 in the revised MS. So, PM1 has not been removed.

Technical corrections

Has been done accordingly in the revised manuscript

86 “to be the most”

Done

150 “border”

Changed

182 “A similar value”

Done

211 latitudes and longitudes, why “s”

“s” removed

232 “viz.” what is the meaning?

“viz.” has been replaced with “like”

239 “gauge”

Changed

282 “24-hour”

Changed

369 “the emission inventory shows”

Changed

388 “15:00” remove “h”

Removed

487 “is not”

Changed

516 “these periods”

Changed

REVIEWER-3

The authors made a good attempt to conduct the monitoring and modeling studies for the selected air pollutants over the study area. However, the current MS should be further improved before it can be reconsidered for the publication in ACP.

We would like to thank the reviewer for providing useful suggestions to refine our manuscript. Other two reviewers have also pointed out many issues to strengthen our work which we have dealt with in the revised version.

Major comments:

1) It is not clear what hypothesis the authors want to test in this study hence the content is quite diluted and is difficult to follow the MS.

Through this study we aim to understand and document the level of air pollution in Lumbini, located in the northern edge of the IPG before Himalayan foothills start to rise, during pre-monsoon (significantly polluted season in the Indo-Gangetic Plains), the diurnal characteristics of various air pollutants, and the influence of open biomass burning on the air quality in Lumbini region.

2) The linkage between the modeling and monitoring parts appear to be quite weak. How the results of both parts supported each other to reach the study objectives (and what are these)? If both monitoring and modeling results are to be incorporated then the purpose/research question should be clearly defined from the beginning.

Modeling work is used only to fill data gaps and understand source regions. We have reduced the scope of the modeling work as suggested by reviewers by removing the chemical compositional analysis. Models are evaluated with observations for improvement in emissions inventory and simulating meteorology parameters. Our analysis will aid in improving emissions work. These are highlighted in the manuscript.

The main objective of this work was to understand the level of air pollution, diurnal characteristics and the influence of open biomass burning on air quality in Lumbini.

In my opinion, it would be more interesting if the authors make better attempt to analyze the monitoring data (including also PM1, O3 etc.) in relation to the sources and meteorology, etc. rather than to loosely cover all the activities/results as presented in this version.

We have tried our best to revise the manuscript by discussing more on the observed PM fractions, their ratios, and BC/PM ratio (please see the response to Reviewer-2). Moreover, a new paragraph on influence of meteorology on concentrations of air pollutants (see also Figure S3) has also been inserted. Please see the Section 3.2.1 **General overview, PM ratios and influence of meteorology on pollution concentrations** in the revised manuscript.

3) The methodology for the modeling part should be described in detail, especially the emission input data. The authors claimed in Line 436 that both modeling and monitoring results showed CO peaks during the biomass burning events but not indicated if and how the emissions from these 2 events were also included in the emission input data.

Section 2.3 does describe the emissions. Anthropogenic emissions are taken from HTAP v2 data while open burning is taken from data from FINN model. Both these emissions are widely used and references for these model/data are cited in the paper. Both emissions are re-gridded to the STEM model domain. Several STEM papers are cited that use this technique. Again due to reviewer's suggestion, the modeling scope of the paper has been reduced to identifying regional sources and filling in data gaps. Thus to go into further model component detail is not warranted.

Minor comments:

1) The description of monitoring instrument (2.2) is lengthy and could be moved to SI.

We have removed the (unwanted) description of monitoring instruments to make the section short and informative.

2) Too many qualitative statements in the MS.

We would like to thank the reviewer for pointing this out. Other reviewer also has pointed the same issue which we have already addressed earlier (please see the responses to the Reviewer-1).

1 **Pre-monsoon air quality over Lumbini, a world heritage site**
2 **along the Himalayan foothills**

3 Dipesh Rupakheti^{1,2*}, Bhupesh Adhikary³, Puppala S. Praveen³, Maheswar Rupakheti^{4,5},
4 Shichang Kang^{6,7*}, Khadak S. Mahata⁴, Manish Naja⁸, Qianggong Zhang^{1,7}, Arnico K. Panday³,
5 Mark G. Lawrence⁴

6 ¹Key Laboratory of Tibetan Environment Changes and Land Surface Processes, Institute of
7 Tibetan Plateau Research, Chinese Academy of Sciences, Beijing 100101, China

8 ²University of Chinese Academy of Sciences, Beijing 100049, China

9 ³International Centre for Integrated Mountain Development (ICIMOD), Kathmandu, Nepal

10 ⁴Institute for Advanced Sustainability Studies (IASS), Potsdam 14467, Germany

11 ⁵Himalayan Sustainability Institute (HIMSI), Kathmandu, Nepal

12 ⁶State Key Laboratory of Cryospheric Science, Cold and Arid Regions Environmental and
13 Engineering Research Institute (CAREERI), Lanzhou 730000, China

14 ⁷Center for Excellence in Tibetan Plateau Earth Sciences, Chinese Academy of Sciences, Beijing
15 100085, China

16 ⁸Aryabhata Research Institute of Observational Sciences (ARIES), Nainital, India

17

18 **Correspondence to:*

19 D. Rupakheti (dipesh.rupakheti@itpcas.ac.cn), S.C. Kang (shichang.kang@lzb.ac.cn)

20

21 Abstract

22 Lumbini, in southern Nepal, is a UNESCO world heritage site of universal value as the
23 birthplace of Buddha. Poor air quality in Lumbini and surrounding regions is a great concern for
24 public health as well as for preservation, protection and promotion of Buddhist heritage and
25 culture. We present here results from measurements of ambient concentrations of key air
26 pollutants (PM, BC, CO, O₃) in Lumbini, first of its kind for Lumbini, conducted during an
27 intensive measurement period of three months (April-June 2013) in the pre-monsoon season. The
28 measurements were carried out as a part of the international air pollution measurement
29 campaign; SusKat-ABC (Sustainable Atmosphere for the Kathmandu Valley - Atmospheric
30 Brown Clouds). **The main objective of this work was to understand and document the level of air
31 pollution, diurnal characteristics and the influence of open biomass burning on air quality in
32 Lumbini. The ranges of hourly average concentrations were: PM₁₀: 10.5–604.0 μg m⁻³, PM_{2.5}:
33 6.1–272.2 μg m⁻³; BC: 0.3–30.0 μg m⁻³; CO: 125.0–1430.0 ppbv; and O₃: 1.0–118.1 ppbv.**
34 **The hourly average concentrations during the entire measurement campaign ranged as follows:
35 BC: 0.3 - 30.0 μg m⁻³, PM₁: 3.6-197.6 μg m⁻³, PM_{2.5}: 6.1 - 272.2 μg m⁻³, PM₁₀: 10.5 - 604.0 μg
36 m⁻³, O₃: 1.0 - 118.1 ppbv, and CO: 125.0 - 1430.0 ppbv.** These levels are comparable to other
37 very heavily polluted sites ~~throughout~~ in South Asia. **Higher fraction of coarse mode PM was
38 found as compared to other nearby sites in the IGP region. ΔBC/ΔCO ratio obtained in Lumbini
39 indicated considerable contributions of emissions from both domestic and transportation sectors.**
40 The 24-h average PM_{2.5} and PM₁₀ concentrations exceeded the WHO guideline very frequently
41 (94% and 85% of the sampled period, respectively), which implies significant health risks for the
42 residents and visitors in the region. These air pollutants exhibited clear diurnal cycles with high
43 values in the morning and evening. During the study period, the worst air pollution episodes
44 were mainly due to agro-residue burning and regional forest fires combined with meteorological
45 conditions conducive of pollution transport to Lumbini. Fossil fuel combustion also contributed
46 significantly, accounting for more than half of the ambient BC concentration according to
47 aerosol spectral light absorption coefficients obtained in Lumbini. WRF-STEM, a regional
48 chemical transport model, was used to simulate the meteorology and the concentrations of
49 pollutants to understand the pollutant transport pathways. The model was able to reproduce the
50 temporal variation in the pollutant concentrations well; however, estimated values were 1.5 to 5
51 times lower than the observed concentrations for CO and PM₁₀ respectively. **Model simulated**

52 regionally tagged CO tracers showed **that** the majority of CO came from the upwind region of
53 Ganges Valley. ~~The model was also used to examine the chemical composition of the aerosol~~
54 ~~mixture, indicating that organic carbon was the main constituent of fine mode PM_{2.5}, followed by~~
55 ~~mineral dust.~~ **Model needs significant improvement in simulating aerosols in the region.** Given
56 the high pollution level, there is a clear and urgent need for setting up a network of long-term air
57 quality monitoring stations in the greater Lumbini region.

58 1. Introduction

59 The Indo-Gangetic plain (IGP) stretches over 2000 km encompassing a vast area of land in
60 northern South Asia: the eastern parts of Pakistan, most of northern and eastern India, southern
61 part of Nepal, and almost all of Bangladesh. The Himalayan mountains and their foothills stretch
62 along the northern edge of IGP. The IGP region is among the most fertile and most intensely
63 farmed region of the world. It is a heavily populated region with about 900 million residents or
64 12% of the world's population. Four megacities - Lahore, Delhi, Kolkata, and Dhaka are located
65 in the IGP region, with dozens more cities with populations exceeding one million. The region
66 has witnessed impressive economic growth in recent decades but unfortunately it has also
67 become one of the most polluted, and an air pollution 'hot spot' of local, regional and global
68 concern (Ramanathan et al., 2007). Main factors contributing to air pollution in the IGP and
69 surrounding regions include emissions from vehicles, thermal power plants, industries, biomass
70 and fossil fuel used in cooking and heating activities, agricultural activities, crop residue burning
71 and forest fires. Air pollution gets transported long distances away from emission sources and
72 across national borders. As a result, the IGP and adjacent regions get shrouded with a dramatic
73 annual buildup of regional scale plumes of air pollutants, known as Atmospheric Brown Clouds
74 (ABC), during the long and dry winter and pre-monsoon seasons each year (Ramanathan and
75 Carmichael, 2008). Figure 1 shows the mean aerosol optical depth (AOD) acquired **from** the
76 MODIS instrument onboard TERRA satellite over South Asia for a period of December 2012-
77 June 2013. Very high aerosol **optical depth** along the entire stretch of IGP reflects severity of air
78 pollution over large areas in the region.

79 Poor air quality continues to pose significant threat to human health in the region. In a new study
80 of global burden of disease released recently, Forouzanfar et al. (2015) estimated that in 2013
81 around 1.7 million people died prematurely in Pakistan, India, Nepal, and Bangladesh as a result

82 of air pollution exposure, nearly 30% of global total premature deaths due to air pollution. Air
83 pollution also affects precipitation (e.g. South Asian monsoon), agricultural productivity,
84 ecosystems, tourism, climate, and broadly socio-economic and national development goals of the
85 countries in the region (Burney and Ramanathan, 2014; Shindell, 2011; Ramanathan and
86 Carmichael, 2008). It has also been linked to intensification of cold wave and winter fog in the
87 IGP region over recent decades (Lawrence and Lelieveld, 2010 and references therein; Safai et
88 al., 2009; Ganguly et al., 2006). Besides high levels of aerosol loading as shown in Fig. 1, Indo-
89 Gangetic plains also have very high levels of ground level ozone or tropospheric ozone (O_3)
90 (e.g., Ramanathan and Carmichael (2008)). It is a toxic pollutant to plant and human health, and
91 a major greenhouse gas (IPCC, 2013; Shindell, 2011; Mohnen et al., 1993). South Asia, in
92 particular IGP region, has been projected to be **the** most ozone polluted region in world by 2030
93 (Stevenson et al., 2006). Majority of crop loss in different parts of the world results from effects
94 of ozone on crop health and productivity (Shindell, 2011). Burney and Ramanathan (2014) **also**
95 reported a significant loss in wheat and rice yields in India from 1980 to 2010 due to direct
96 effects of black carbon (BC) and ozone (O_3). BC and O_3 are two key short-lived climate
97 pollutants (SLCP). Because of the IGP's close proximity to the Himalaya-Tibetan plateau region,
98 this once relatively clean region, is now subjected to increasing air pollution transported from
99 regions such as the IGP, which can exert additional risks to sensitive ecosystems in the mountain
100 region (e.g., (Lüthi et al., 2015; Marinoni et al., 2013; Duchi et al., 2011). Air pollution transport
101 pathways to Himalayas are still not yet fully understood.

102 ~~Air pollution can also damage the built environment and cultural and archeological heritages~~
103 ~~(Brimblecombe, 2003)~~. Monuments and buildings made with stones are vulnerable to air
104 pollution damage (Brimblecombe, 2003; Gauri and Holdren, 1981). Sulfur dioxide, which forms
105 sulfuric acid upon reaction with water is the most harmful substance for the monuments as it can
106 corrode and damage them (Baedecker et al., 1992; Gauri and Holdren, 1981). Indo-Gangetic
107 plains are rich in archeological, cultural and historical sites and monuments and many of them
108 are inscribed as UNESCO World Heritage Site. For example, among many other such sites in
109 IGP are the Archaeological Ruins at Moenjodaro (Pakistan), Taj Mahal in Agra and Mahabodhi
110 Temple Complex in Bodh Gaya (India), Lumbini (Nepal), and ruins of the Buddhist Vihara at
111 Paharpur (Bangladesh) (World Heritage List; UNESCO, website: <http://whc.unesco.org/en/list>).
112 The Taj Mahal is one of the seven wonders of the modern world and India's greatest landmark.

113 ~~Starting in 1970s, there have been observations of brownish/yellowish tone on its shiny~~
114 ~~white marble façade, and the primary suspect of discoloration was heavy air pollution from~~
115 ~~industries and traffic that grew around the monument site in Agra over the past decades. At the~~
116 ~~end of the last century, the government of India realized the growing problem of air pollution~~
117 ~~damage to the Taj Mahal and started a program to save the monument. It introduced measures to~~
118 ~~cut back pollution, as well as set up stations around the monument to monitor air quality around~~
119 ~~the clock.~~ A recent study has reported that deposition of light absorbing aerosol particles (black
120 carbon, brown carbon) and dust is responsible for its discoloration (Bergin et al., 2015).

121 Lumbini, located near the northern edge of the central Ingo-Gangetic plain, is famous as the
122 birthplace of the Lord Buddha. Lumbini is a UNESCO world heritage site of outstanding
123 universal value to humanity, inscribed in the UNESCO list since 1997. The site, with valuable
124 archaeological remains of the Buddhist *Viharas* (monasteries) and *Stupas* (memorial shrines), as
125 well as modern temples and monasteries, is a center of attraction and visited by hundreds of
126 thousands of pilgrims, scientists, scholars, yogis, and tourists every year. ~~Over recent years, there~~
127 ~~is increasing concern about poor air quality in Lumbini and the surrounding region.~~ There ~~was~~ is
128 no **regular air quality monitoring** ~~surface monitoring of air quality in Lumbini at the time of our~~
129 **measurement campaign.**

130 **Through this study, we want to understand the level of air pollution, its diurnal characteristic,**
131 **and the influence of open biomass burning on air quality in Lumbini.** ~~As a first attempt to~~
132 ~~understand air quality in Lumbini,~~ We carried out continuous measurements of ambient
133 concentrations of key air pollutants (particulate matter, black carbon, carbon monoxide, ozone)
134 and meteorological parameters ~~other auxiliary measurements (Aerosol optical depth not~~
135 ~~discussed on the present study, meteorological parameters)~~ during an intensive measurement
136 period of three months (April-June) in the year 2013. These are the first reported pollutant
137 measurements for Lumbini. A regional chemical transport model called Sulfur Transport and
138 dEposition Model (STEM) was used to simulate the variations of meteorological parameters and
139 air pollutants during the observation period **to understand pollution source region as well as the**
140 **contribution of open biomass burning to air quality in Lumbini. Model simulated** regionally
141 tagged CO tracers were used to identify emission source regions impacting pollutant
142 concentration observed at Lumbini. Satellite data has also been used to understand the high

143 pollution events during the monitoring period. These measurements were carried out as a part of
144 the SusKat-ABC international air pollution measurement campaign (*M. Rupakheti, manuscript in*
145 *preparation for ACPD*) jointly led by the International Centre for Integrated Mountain
146 Development (ICIMOD), Kathmandu, Nepal and Institute for Advanced Sustainability Studies
147 (IASS), Potsdam, Germany.

148 2. Experimental set up

149 2.1 Sampling site

150 The Lumbini measurement site (27°29.387' N, 83°16.745' E, elevation: ~100 m above sea level)
151 is located at the premise of the Lumbini International Research Institute (LIRI), a Buddhist
152 library in Lumbini. Lumbini lies in the Nepal's southern lowland plain or *Terai* region, termed as
153 "bread basket of Nepal" due to the availability of very fertile land suitable for crop production,
154 which forms the northern edge of the Indo-Gangetic Plains (IGP). 25 km north of Lumbini the
155 foothills begin, while the main peaks of the Himalayas are 140 km to the north. The remaining
156 three sides are surrounded by flat plain land of Nepal and India. The site is only about 8 km from
157 the Nepal-India ~~border~~ border in the south. A three storied 10 m tall water tower was used as
158 the platform for the automatic weather station (AWS) whereas remaining instruments were
159 placed inside a room near the base of the tower. Figure 2 shows the location of Lumbini, the
160 Kenzo Tange Master Plan area of the Lumbini development project, and the sampling tower. An
161 uninterrupted power back up was set up in order to assure the regular power supply even during
162 hours with scheduled power cuts during the monitoring period. The nearby premises of the
163 monitoring site consist of the LIRI main office and staff quarters. Further away is a museum, a
164 local bus park for the visitors to Lumbini, the office of the Lumbini Development Trust,
165 monasteries, and thinly forested area with grassland within the master plan area. Outside of the
166 master plan area lie vast area of agricultural fields, village pockets, and several brick kilns and
167 cement industries. A local road (black topped), that cuts through the master plan area, lies about
168 200 m north of the sampling site and experiences intermittent passing of vehicles. According to
169 the Ministry of Culture, Tourism and Civil Aviation of Nepal over 130 thousand tourists
170 (excluding Nepalese and Indian citizens) visited the Lumbini area in 2014
171 (<http://tourism.gov.np/en>).

172 2.2 Monitoring Instruments

173 The summary of instruments deployed in Lumbini is presented in Table 1. ~~They monitored~~
174 ~~ambient concentrations of various air pollutants and local meteorological parameters~~
175 ~~continuously during the sampling period of about two and half months.~~ All data were collected in
176 Nepal Standard Time (NST) which is GMT +05:45 hour. PM₁, PM_{2.5} and PM₁₀ mass
177 concentrations were monitored continuously with GRIMM EDM164 (GRIMM Aerosol Technik,
178 Germany), ~~reporting data every 5 min. The instrument~~ **which** uses the light scattering at 655 nm
179 to derive mass concentrations. ~~More description on the technical aspects of the instrument can be~~
180 ~~found on the manufacturer's website ([http://wiki.grimm-aerosol.de/index.php?title=ENVIRO-](http://wiki.grimm-aerosol.de/index.php?title=ENVIRO-EDM164)~~
181 ~~[EDM164](http://wiki.grimm-aerosol.de/index.php?title=ENVIRO-EDM164)).~~ The EDM164 used in this study was a newly purchased instrument which was
182 calibrated at the factory of the GRIMM Aerosol Technik in Germany before it was deployed at
183 Lumbini. Similarly, aerosol light absorptions at 7 wavelengths (370, 470, 520, 590, 660, 880,
184 950 nm) were measured continuously with an Aethalometer (Model AE-42, Magee Scientific,
185 USA), averaging and reporting data every 5 min. ~~AE-42~~ **It** was operated at a flow rate of 5 l min⁻¹
186 **¹. No cut-off was applied for inlet; hence the reported concentration of BC is total suspended BC**
187 **particles.** As described by the manufacturer, ambient BC concentration is derived from light
188 absorption at 880 nm using a specific mass absorption cross section. To obtain BC concentration
189 in Lumbini, we used a specific mass absorption cross-section value of 8 m² g⁻¹ for the 880 nm
190 channel. **A** similar value has been previously used for BC measurement in the Indo-Gangetic
191 plain (Praveen et al., 2012). ~~Optical measurement by filter based absorption photometers, such as~~
192 ~~the Aethalometer, suffer from measurement artifact known as filter loading effect which must be~~
193 ~~taken into account and corrected for while deriving ambient BC concentrations.~~ **To remove the**
194 **filter loading effect, we** used correction method suggested by Schmid et al. (2006) which was
195 also used by Praveen et al. (2012) for BC measurements at a rural site in the Indo-Gangetic plain.
196 Surface ozone (O₃) concentration was measured continuously with an ozone analyzer (Model
197 49i, Thermo Scientific, USA), ~~reporting data every minute. It~~ **which** utilizes UV (254 nm
198 wavelength) photometric technology to measure ozone concentration in ambient air. CO analyzer
199 (Model 48i, Thermo Scientific, USA) was used to monitor ambient CO concentration, ~~recording~~
200 ~~data every minute. The CO analyzer~~ **which** is based on the principle that CO absorbs infrared
201 radiation at the wavelength of 4.6 microns. The ambient air was drawn through 6-micron pore
202 size SAVILLEX 47 mm filter at the inlet in order to remove the dust particles before sending air

203 into the CO and O₃ analyzers using a Teflon tube. The filters were replaced every 7-10 days
204 depending on particle loading, based on manual inspection. ~~Both CO and O₃ analyzers were new~~
205 ~~instruments, freshly calibrated at the factory before deploying them in Lumbini.~~ The CO
206 instrument was set to auto-zero at a regular interval of 6 hours. Local meteorological parameters
207 (temperature, relative humidity, wind speed, wind direction, precipitation, and global solar
208 radiation) were monitored with an automatic weather station (AWS) (Campbell Scientific,
209 Loughborough, UK), recording data every minute.

210 **2.3 Regional chemical transport model**

211 Aerosol and trace gas distributions were simulated using a regional chemical transport model.
212 Sulfur Transport and dEposition Model (STEM), a 3D eulerian model, that has been used
213 extensively in the past to characterize air pollutants in South Asian region was used to interpret
214 observations at Lumbini (Kulkarni et al., 2015; Adhikary et al., 2007). The Weather Research
215 and Forecasting (WRF) model (Skamarock et al., 2008) version 3.5.1 was used to generate the
216 required meteorological variables necessary for simulating pollutant transport in STEM. The
217 model domain was centered at 24.94° N latitude and 82.55° E longitude covering a region from
218 3.390° N to 43.308° N ~~latitudes~~ **latitude** and 34.880° E to 130.223° E ~~longitudes~~ **longitude**. The
219 model has 425×200 horizontal grid cells with grid resolution of 25×25 km and 41 vertical layers
220 with top of the model set at 50 mbar. The WRF model was run from November 1, 2012 to June
221 30, 2013. However, for this study, modeled data only from April to June 2013 have been used.
222 The WRF model was initialized with FNL data available from NCAR/UCAR site
223 (<http://rda.ucar.edu/datasets/ds083.2/>).

224 The tracer version of the STEM model provides mass concentration of sulfate, BC (hydrophilic
225 and hydrophobic), Organic carbon (OC), sea salt (fine and coarse mode), dust (fine PM_{2.5} and
226 PM₁₀), CO (biomass and anthropogenic) and region tagged CO tracers. STEM model domain
227 size, resolution and projection are those of the WRF model. Details about tracer version of the
228 STEM model is outlined elsewhere (Kulkarni et al., 2015; Adhikary et al., 2007).
229 Anthropogenic emission of various pollutants (CH₄, CO, SO₂, NO_x, NMVOC, NH₃, PM₁₀,
230 PM_{2.5}, BC and OC) used in this analysis were taken from the EDGAR-HTAP_v2
231 (http://edgar.jrc.ec.europa.eu/htap_v2/index.php?SECURE=123). ~~Emission inventory were~~
232 ~~developed for the year 2010 gridded at the spatial resolution of 0.1°×0.1°.~~ Open biomass burning

233 emissions on a daily basis during the simulated period were taken from data obtained from the
234 FINN model (Wiedinmyer et al., 2011). Both these emissions were re-gridded to the STEM
235 model domain. As with the WRF model, the STEM model was run from November 2, 2012 to
236 June 30, 2013 however, data presented here are only during the intensive field campaign period.

237 3. Results and discussions

238 3.1 Meteorology

239 ~~3.1.1 Time series of local meteorological parameters~~

240 Hourly average time series of various meteorological parameters viz. like precipitation in mm hr⁻¹
241 (Prec), temperature in °C (T), relative humidity in % (RH), temperature in °C (T), wind speed
242 in m s⁻¹ (WS) and direction in degree (WD) and wind speed in m s⁻¹ (WS) during the monitoring
243 period are shown in Figure 3. Meteorological parameters were obtained with the sensors at the
244 height of ~12 m from the ground. Moreover, Meteorology results from simulations using a 3D
245 WRF model have been used to compare with the observations, and to fill the data gaps.
246 Precipitation data was derived from TRMM satellite (TRMM_3B42_007 at a horizontal
247 resolution of 0.25°) from the Giovanni platform (<http://giovanni.gsfc.nasa.gov/giovanni/>) as the
248 rain gauge rain gauge malfunctioned during the sampling period. Precipitation data from TRMM
249 (Figure 3) show that Lumbini was relatively dry in the early portion of the measurement
250 campaign while as the pre-monsoon edged closer to the monsoon onset, the site did experience
251 some rainfall events. This lowered aerosol loading in the later half of the measurement campaign
252 due to washout. Comparison of WRF model outputs with TRMM data shows that the model
253 under-predicts rainfall through out the campaign.

254 Average observed temperature for the sampling period until the sensor stopped working (on 8th
255 May, 2013, i.e., for 38 days of measurement) was 28.1°C (minimum: 16.5°C, maximum: 40°C).
256 Average temperature from the model, during same period, was 31°C with values ranging
257 between 19 - 40°C. As shown in Figure 3, the model captures the synoptic variability of
258 temperature and is mostly within the range of daily values. However, the model has a high bias
259 and does not capture well daily minimum temperature values. The model does not show any
260 large variation in temperature for the period after the sensors stopped working. This insight will
261 be useful to interpret pollution data later on.

262 For the same period (until the sensor stopped working), the average (observed) RH was ~ 50%
263 (ranging from 10.5 to 97.5%) whereas the model showed the average RH to be ~ 23% with
264 values ranging between 6 to 78%. RH values are highly underestimated by the model however;
265 the synoptic scale variability is captured by the model.

266 Average observed wind speed during the study period was 2.4 m s^{-1} , with hourly values ranging
267 between $0.03 - 7.4 \text{ m s}^{-1}$ whereas from the WRF model average wind speed was found to be 3.2
268 m s^{-1} (range: $0.06 - 11.1 \text{ m s}^{-1}$). ~~Comparison of the model output data with observation shows~~
269 ~~that the model adequately captures wind speed to study pollutant transport.~~ Diurnal variation of
270 observed hourly average wind speed suggested that wind speeds were lower during nights and
271 mornings while higher wind speed prevailed during day time, with average winds $> 3 \text{ m s}^{-1}$ up to
272 $\sim 3.3 \text{ m s}^{-1}$ between 09:00-13:00 local time (Supplementary materials, Figure S1, ~~upper~~ lower
273 panel). High speed strong winds ($> 4 \text{ m s}^{-1}$) were from the NW direction during the month of
274 April which later switched to almost opposite direction, i.e., SE direction from the month of May
275 onwards. Figure 4 shows the monthly wind rose plot (using WRPLOT view from the Lakes
276 Environmental, <http://weblakes.com/>). Comparing modeled wind direction prediction skills at the
277 surface with one point measurement is not sufficient. However, in the absence of other
278 measurements, we also show the comparison of wind direction. Since there are no glaringly
279 large biases in the observed surface wind direction, and the lack of measured upper wind data
280 even from nearby region, we use the model to interpret pollutant transport to Lumbini. ~~Average~~
281 ~~observed temperature for the sampling period until the sensor stopped working (on 8th May,~~
282 ~~2013, i.e., for 38 days) was 28.1°C , with a minimum value recorded to be 16.5°C whereas the~~
283 ~~maximum was 40°C . Average T from the model, during same period, was 31°C with values~~
284 ~~ranging between $19 - 40^{\circ}\text{C}$. The model captures the synoptic variability of temperature and is~~
285 ~~mostly within the range of daily values. However, the model has a high bias and does not~~
286 ~~capture daily minimum temperature values. For the same period (until the sensor stopped~~
287 ~~working), the average (observed) RH was ~ 50% (ranging from 10.5 to 97.5%) whereas the~~
288 ~~model showed the average RH to be ~ 23% (same period as observation) with values ranging~~
289 ~~between 6 to 78%. RH values are highly underestimated by the model however; the synoptic~~
290 ~~scale variability is captured by the model.~~ Discrepancy on model results might have occurred
291 due to various factors inherently uncertain in a weather model. However, we believe that

292 modeled data is vital for understanding pollutant transport in an area where observation data are
293 non-existent or are incomplete.

294 **3.1.2** ~~Synoptic scale winds during pre-monsoon~~

295 The monthly mean synoptic wind for the month of April, May and June is presented in Figure 5.
296 NCEP/NCAR reanalysis monthly data of winds at 1000 mbar were used to study the wind
297 pattern. The red dot in the figure indicates the location of Lumbini. NCEP/NCAR data showed
298 the dominance of calm winds over the measurement site. Similar type of wind directions were
299 observed over Kanpur, India, also in the IGP, during the pre-monsoon season (Srivastava et al.,
300 2011).

301 **3.2 Time-series of air pollutants Air Quality**

302 **3.2.1 General overview, PM ratios and influence of meteorology on pollution** 303 **concentrations**

304 ~~Figure 6 shows hourly averaged time-series of both observed and modeled PM₁₀, PM_{2.5}, BC, CO~~
305 ~~and O₃ observed at Lumbini during the study period. In this section, results have been discussed~~
306 ~~based upon the observation datasets only. Section 3.2.3 will discuss model comparison and~~
307 ~~interpretation.~~

308 ~~*Both PM fractions:* PM₁₀ and PM_{2.5} showed similar temporal behavior. Observed hourly average~~
309 ~~PM₁₀ concentrations ranged between 10.5–603.9 $\mu\text{g m}^{-3}$ with an average of $128.9 \pm 91.9 \mu\text{g m}^{-3}$~~
310 ~~whereas PM_{2.5} concentrations ranged between 6.1 and 272.2 $\mu\text{g m}^{-3}$ with an average of 53.1 ± 35.1~~
311 ~~$\mu\text{g m}^{-3}$ during the sampling period. In addition to this, average PM₁ concentration was 35.8 ± 25.6~~
312 ~~$\mu\text{g m}^{-3}$ with the concentrations ranging between 3.6 to 197.6 $\mu\text{g m}^{-3}$. PM₁ concentration has not~~
313 ~~been discussed in this study. The observed 24-hour average particulate matter concentrations~~
314 ~~(PM_{2.5} and PM₁₀) were found frequently higher than the WHO-prescribed guidelines for PM_{2.5}~~
315 ~~(25 $\mu\text{g m}^{-3}$) and PM₁₀ (50 $\mu\text{g m}^{-3}$), (WHO, 2006) — PM_{2.5}: 94% and PM₁₀: 85% of the~~
316 ~~measurement period of 53 days. Similarly, BC concentrations during the measurement period~~
317 ~~ranged between 0.3–29.9 $\mu\text{g m}^{-3}$ with a mean (\pm SD) value of $4.9 (\pm 3.8) \mu\text{g m}^{-3}$. The lowest~~
318 ~~concentration was observed during a rainy day (21–22 April) whereas the highest concentration~~
319 ~~was observed during a period of forest fire (detailed in Section 3.4). BC concentrations in~~

320 Lumbini during pre-monsoon months are lower compared to BC concentrations observed in the
321 Kathmandu Valley because of high number of vehicles plying on the street, brick kilns and other
322 industries in Kathmandu valley (Putero et al., 2015a; Sharma et al., 2012).

323 Figure 6 shows hourly averaged time series of observed BC, PM₁, PM_{2.5}, PM₁₀, CO and O₃
324 observed at Lumbini during the study period. Similar temporal behaviour was shown by BC,
325 particulate matter fractions (PM₁, PM_{2.5} and PM₁₀) and CO. BC concentrations during the
326 measurement period ranged between 0.3-29.9 µg m⁻³ with a mean (±SD) value of 4.9 (±3.8) µg
327 m⁻³. BC concentrations in Lumbini during pre-monsoon months are lower compared to BC
328 concentrations observed in the Kathmandu Valley because of high number of vehicles plying on
329 the street, brick kilns and other industries in Kathmandu valley (Sharma et al., 2012; Putero et
330 al., 2015b). The lowest concentration was observed during a rainy day (21-22 April) whereas the
331 highest concentration was observed during a period of forest fire (detailed in Section 3.4). For
332 the entire measurement period, we found average (of hourly average values) PM₁: 35.8±25.6 µg
333 m⁻³ (minimum-maximum range: 3.6 - 197.6 µg m⁻³), PM_{2.5}: 53.1±35.1 µg m⁻³ (6.1 - 272.2 µg m⁻³),
334 PM₁₀: 128.9±91.9 µg m⁻³ (10.5-603.9 µg m⁻³) and coarse-mode (PM_{10-2.5}): 75.65±61.67 µg m⁻³
335 (1.98-331.80 µg m⁻³). The coarse-mode fraction was ~ 60% of the PM₁₀. The share of coarse-
336 mode aerosol to PM₁₀ in Lumbini was higher than that observed in other sites in the IGP;
337 Guwahiti, India (42%) (Tiwari et al., 2017) and Dibrugarh, India (9-16%) (Pathak et al., 2013)
338 both in eastern IGP and Delhi (38%) (Tiwari et al., 2015) in western IGP indicating the higher
339 contribution of coarse aerosols in Lumbini, likely lifted from soils from nearby agricultural fields
340 and construction materials by stronger winds during pre-monsoon season. Similar value of
341 coarse-mode fraction, as in Lumbini, has been reported by Misra et al. (2014) at Kanpur for dust
342 dominated and mixed aerosols events.

343 The share of BC in PM fractions were found to be ~13% in PM₁, 9% in PM_{2.5} and ~4% in PM₁₀
344 but the correlation coefficients of BC with three PM fractions were found to be 0.89 (PM₁), 0.88
345 (PM_{2.5}) and 0.69 (PM₁₀), indicating the commonality in the sources of these pollutants. The
346 contribution of BC in PM₁ was found to be of ~12% in Kanpur during February-March (Kumar
347 et al., 2016a) similar to Lumbini. Regarding the share of BC in PM₁₀, the share observed in
348 Lumbini (~4%) was similar to that observed over Varanasi (~340 km due south of our site) in
349 central IGP (5%) (Tiwari et al., 2016) and Dibrugarh in eastern IGP (~5%) (Pathak et al., 2013).

350 Thus our results indicate that despite our station being located at the northern edge of the IGP
351 along the foothills of the Himalayan range, its aerosol characteristics are similar to those found in
352 heavily polluted sites in the central and eastern IGP.

353 In Lumbini, the average (hourly) share of PM_1 in $PM_{2.5}$, PM_1 in PM_{10} and $PM_{2.5}$ in PM_{10} were
354 found to be ~70%, 34% and 47% respectively. The share of average (sampling period) coarse-
355 mode aerosols to PM_{10} (60%) was found to be higher as compared to that of average fine mode
356 i.e., $PM_{2.5}$ (40%). Regarding other sites in IGP region, $PM_{2.5}/PM_{10}$ ratios were reported to be
357 56% in Kanpur (Snider et al., 2016), 60% in Varanasi (Kumar et al., 2015), 57% in Guwahati
358 (Tiwari et al., 2017), 90% in Dribugarh (Pathak et al., 2013) and 62% in Delhi (Tiwari et al.,
359 2015) indicating local differences within IGP as well as suggesting that influence of combustion
360 sources at Lumbini is still lower compared to other locations in Indian section of the IGP. A
361 recent study (Putero et al., 2015b) reported the PM_1/PM_{10} during pre-monsoon of 2013 was
362 found to be 0.39 in the Kathmandu Valley of Nepal. Lumbini has significantly lower vehicle
363 emissions and human population than the Kathmandu Valley yet the ratios are similar, indicating
364 the importance of regional combustion sources in Lumbini for finer aerosols (PM_1), and soil-
365 based emissions such as road dust in the Kathmandu Valley. Future studies will need to explore
366 the emission sources around Lumbini in much greater detail. Lower $PM_{2.5}/PM_{10}$ in Lumbini as
367 compared to other regions mentioned earlier could be due to emissions from cement industries
368 located within 15 km distance from the measurement site. Cement factories emit coarse sized
369 particles but we are not able to distinguish in our measurement without having an analysis of
370 certain marker species. Trivedi et al. (2014) reported a ratio of 0.39 (during pre-monsoon) over
371 Delhi, which is lower than the ratio in Lumbini. The lower ratio in Delhi was due to the presence
372 of coarse sized windblown desert dust and suspended soil materials due to strong winds.

373 The observed 24-hour average particulate matter concentrations ($PM_{2.5}$ and PM_{10}) were found
374 frequently higher than the WHO prescribed guidelines for $PM_{2.5}$ ($25 \mu g m^{-3}$) and PM_{10} ($50 \mu g m^{-3}$)
375 with $PM_{2.5}$: exceeding 94% and PM_{10} : 85% of the measurement period of 53 days.

376 Observed CO concentrations ranged between 124.9-1429.7 ppbv with an average value of
377 344.1 ± 160.3 ppbv. CO concentration observed in Lumbini is lower than that of Mohali, Western
378 India where the average concentration was 566.7 ppbv during pre-monsoon season due to intense
379 biomass and agro-residue burning over the region (Sinha et al., 2014). Temporal variation of CO

380 concentrations is similar to that of BC as both of these species are emitted during incomplete
381 combustion of fuel. Moreover, a very strong correlation ($r = 0.9$) was observed between BC and
382 CO. Past studies have shown that the ratio of BC to CO depends upon multiple factors like site
383 location, combustion characteristics (fuel and technology) at the sources, and type of air mass
384 (Girach et al., 2014; Pan et al., 2011; Zhou et al., 2009). Formation of the soot depends on the
385 carbon to oxygen ratio of fuel whereas CO can also be produced naturally due to the oxidation of
386 VOCs (Girach et al., 2014). Figure 7 shows the comparison of the average $\Delta BC/\Delta CO$ ratio
387 (0.021) at Lumbini with that obtained from other sites. Please refer to Figure S2 in the
388 supplementary materials for the time series of $\Delta BC/\Delta CO$ ratio observed in Lumbini. We used the
389 method described by Pan et al. (2011) to calculate the $\Delta BC/\Delta CO$ values. The ratio was
390 calculated using the equation $(BC-BC_0)/(CO-CO_0)$ assuming the background values (BC_0 or
391 CO_0) as 1.25 percentile of the data. The $\Delta BC/\Delta CO$ ratio in Lumbini is similar to that obtained at
392 a suburban site, Pantnagar in India (0.017) (Joshi et al., 2016) and in Maldives (0.017)
393 (Dickerson et al., 2002). As compared to Lumbini, the different $\Delta BC/\Delta CO$ ratio obtained over
394 megacities such as Beijing and Shanghai are due to the higher number of gasoline and diesel
395 vehicles (Zhou et al., 2009). However, the ratio obtained at Lumbini were within the range of
396 emission ratios from diesel used in transport sector (0.0013-0.055), coal (0.0019-0.0572) and
397 biofuels (0.0087-0.0266) for domestic activities (Verma et al., 2010 and references therein). ~~BC~~
398 ~~to CO ratio in Lumbini was found to be different from that observed at other urban and rural sites~~
399 ~~and those affected by forest fire/biomass burning. However, a sub-urban site, Pantnagar, in IGP~~
400 ~~also observed similar BC to CO ratio (Joshi et al., 2016) as observed in Lumbini. There was a~~
401 ~~very strong correlation ($r > 0.9$) between BC and CO (Supplementary material, Figure S2),~~
402 ~~indicating likely common sources of emission for both pollutants.~~ The hourly averaged observed
403 ozone concentration ranged between 1.0 and 118.1 ppbv with a mean value of 46.6 ± 20.3 ppbv
404 during the sampling period. The 8-hr maximum O_3 concentration exceeded WHO guidelines of
405 $100 \mu g m^{-3}$ (WHO, 2006) during 88% of the measurement period. Our results clearly indicate
406 that the current pollution levels in Lumbini is of great concern to health of the people living in
407 the region as well as over a million visitors who visit Lumbini, as well as ecosystems,
408 particularly agro-ecosystem, especially in warm and sunny pre-monsoon months.

409 The relationship of wind speed (WS) with aerosol and gaseous pollutants in Lumbini is shown in
410 Figure S3 (Supplementary information). We were interested in studying the relationship between

411 wind speed and the pollutants since the wind governs the horizontal dilution of the pollutants
412 (Huang et al., 2012) and also likelihood of lifting soil dust. Except ozone, all other pollutants
413 exhibited negative correlation with wind speed. BC shows negative correlation ($r = -0.42$) with
414 the wind speed which is similar with other pollutants as well (as can be seen from the figure).
415 Past studies have also reported a similar negative correlation of BC with wind speed over urban
416 and sub-urban areas (Huang et al., 2012; Cao et al., 2009; Ramachandran and Rajesh, 2007;
417 Sharma et al., 2002; Tiwari et al., 2013) indicating that the locally generated BC can accumulate
418 in the atmosphere during lower wind speed conditions (Cao et al., 2009). Tiwari et al. (2013)
419 also reported similar negative correlation ($r = -0.45$) during the pre-monsoon season over Delhi.
420 On the other hand, secondary pollutants like ozone exhibited a positive relation with the WS
421 ($r=0.38$) indicating the WS could be one of the potential factors of high ozone in Lumbini. Solar
422 radiation is one of the most important factors for production of ozone in the atmosphere (Naja et
423 al., 2003). The correlation of hourly ozone concentration with solar radiation (not shown here)
424 was found to be 0.41 whereas wind speed during the daytime only (06:00-18:00) showed very
425 weak correlation of 0.02 with ozone, indicating the calm condition as conducive to formation and
426 accumulation of ozone in the region.

427 Interestingly, the highest concentrations of all measured pollutants were obtained when the wind
428 speed was less than 1 m s^{-1} . In a separate analysis (not shown here), we considered only the WS
429 $>1 \text{ m s}^{-1}$ and calculated the correlation coefficients to investigate the influence of regional
430 emissions. We found the similar correlation values as previous when all WS values were
431 considered (BC vs WS = -0.41, CO vs WS = -0.42, O₃ vs WS= 0.29, PM₁ vs WS= -0.40, PM_{2.5}
432 vs WS= -0.38, PM₁₀ vs WS= -0.33). The correlation of WS ($>1 \text{ m/s}$) with concentration of air
433 pollutants elucidates that air pollution over Lumbini is not only of the local origin, it is rather
434 transported from other nearby regions as well.

435 Past studies near this site have been focused on the cities like Kathmandu (Sharma et al., 2012;
436 Ram et al., 2010; Panday and Prinn, 2009; Putero et al., 2015b) and Kanpur (Ram et al., 2010)
437 and agro-residue burning dominated regions of IGP (Rastogi et al., 2016; Sinha et al., 2014;
438 Sarkar et al., 2013) or a remote mountain location in India (Naja et al., 2014). Very high aerosol
439 loading is observed in South Asia during pre-monsoon, mostly over the IGP region
440 (Supplementary materials, [Figure S4](#)). ~~In order to put our results in perspective, pollution levels~~
441 ~~observed in Lumbini have been compared with the observations from other sites in the region~~

442 and are presented in Table 2. As this is the first study over an IGP site located in Nepal, pollution
443 concentrations observed at Lumbini were compared with other sites in the region (Table 2).
444 Different sites located at urban, semi-urban and remote locations were used for comparison to
445 get a clear comparative picture of the situation at Lumbini amongst other locations in the region.
446 $PM_{2.5}$ concentration in Lumbini have been found to be lower than the megacity like Delhi (Bisht
447 et al., 2015) and north-western IGP regions (Sinha et al., 2014) due to higher level of emissions
448 (from traffic and biomass burning respectively) over those regions. Pre-monsoon seasonal
449 average $PM_{2.5}$ concentration in Lumbini has been found to be lower than the megacity like Delhi
450 (Bisht et al., 2015) and north-western IGP (Sinha et al., 2014), possibly due to higher level of
451 emissions (from traffic and biomass burning, respectively) over those regions. BC concentrations
452 observed in Lumbini during pre monsoon season was lower than the urban Asian cities like
453 Kathmandu (Putero et al., 2015a) and Delhi (Bisht et al., 2015), slightly higher than in Kanpur
454 but high compared to the remote locations in the region. BC observed at Lumbini was higher by
455 a factor of ~6 and ~4.5 compared to that at Mt. Abu, India (Das and Jayaraman, 2011) and near
456 the base of Mt. Everest, Nepal (Marinoni et al., 2013) respectively. Regarding CO, concentration
457 in Lumbini was ~1.5-5 times lower than other urban locations in India (Gaur et al., 2014; Sinha
458 et al., 2014). However, Lumbini CO concentrations are ~2.3-2.6 times higher than nearby remote
459 location such as Mt. Abu (Naja et al., 2003). Average O_3 concentrations, over sampling period,
460 in Lumbini were found to be higher than the cities like Kathmandu (Putero et al., 2015a).
461 However, ozone concentrations higher than that observed at Lumbini were reported at nearby
462 city of Kanpur during pre monsoon season (Gaur et al., 2014). Interestingly ozone
463 concentrations higher than that at Lumbini were observed in the Mt. Everest region. Uplift of the
464 polluted air masses (Marinoni et al., 2013), stratospheric intrusion (Cristofanelli et al., 2010) and
465 even the regional or long-range transport of the air pollutants (Bonasoni et al., 2010) might have
466 contributed for the higher ozone concentration over the Everest region, resulting in higher O_3
467 concentration compared to Lumbini. In addition, average BC and CO concentrations in Lumbini
468 were found falling in between concentrations observed at rural sites (up to 6 times higher) and
469 cities in the region (see Table 2), indicating that Lumbini can still be considered as semi-urban
470 location. The hourly average O_3 concentration in Lumbini were found to be higher than the cities
471 like Kathmandu (Putero et al., 2015b) and Kanpur during pre-monsoon season (Gaur et al.,
472 2014). However from a mesoscale perspective, the hourly average O_3 concentrations were lower

473 at Lumbini as compared to base camp of Mt. Everest region due to the uplift of polluted air
474 masses (Marinoni et al., 2013), stratospheric intrusion (Cristofanelli et al., 2010) and even the
475 regional or long-range transport of the air pollutants (Bonasoni et al., 2010) to the high altitude
476 site.

477 Regarding the monthly average concentration, the concentrations of all measured pollutants
478 decreased as the pre-monsoon months advanced. The monthly average concentrations of the
479 monitored species are shown in the Figure S5 along with the monthly fire hotspots over the
480 region. Reduction in concentration (except PM) during the month of May (as compared to April)
481 could be attributed to the fewer fire events during May as well as previously discussed washout
482 by rainfall. Two peak pollution episodes were observed during the first half of April and May
483 which is discussed in more detail in the next section.

484 3.2.2 Observation-model inter-comparison

485 Chemical transport models provide insight to observed phenomena; however, interpretation has
486 to take into account model performance before arriving at any conclusion. This section describes
487 pollution concentrations simulated by the WRF-STEM model. A comparison of model calculated
488 pollutant concentration along with the minimum and maximum concentrations of various
489 pollutants (with observation) is shown in Table 3. The model based concentrations used here are
490 instantaneous values for every third hour of the day. BC concentrations ranged between 0.4-3.7
491 $\mu\text{g m}^{-3}$ with a mean value of $1.8 \pm 0.7 \mu\text{g m}^{-3}$ for a period of 1st April-15th June 2013. The average
492 model BC concentration was ~ 2.7 times lower than the observed BC. Regarding PM_{10} , $\text{PM}_{2.5}$ and
493 PM_{10} , the model simulated average concentration was 12.3 ± 5.5 (0.9-41.7) $\mu\text{g m}^{-3}$, 17.3 ± 6.7 (1.9-
494 48.3) $\mu\text{g m}^{-3}$ and 25.4 ± 12.9 (2.1-68.8) $\mu\text{g m}^{-3}$, respectively. The model estimated values were
495 lower by the factor of 3 and 5 respectively than the observed concentrations. The data show that
496 model needs much improvement in its ability to adequately predict observed aerosol
497 characteristics. Since pollutant concentration is a function of emissions, transport and
498 transformation and deposition, improvements in any of these areas would improve the model.
499 However, given observation insights by PM ratios, it seems that improvements are much needed
500 in the emissions of primary aerosols. Current emissions does not account for trash burning,
501 roadside dust and increasing newer industries, especially emissions from cement factories that
502 have propped up in recent years.

503 Similarly, Average **observed** CO concentration was 255.7 ± 83.5 ppbv, ranging between 72.2-
504 613.1 ppbv, with average model CO ~ 1.35 times lower than observed. **Comparison of modeled**
505 **CO versus observation is shown in Figure 6. Apart from two peak episodes the model does a**
506 **better job in predicting CO concentration over Lumbini.** Previous study using the STEM model
507 over Kathmandu valley showed **that** the model was able to capture annual BC mean value but
508 completely missed the concentrations during pre-monsoon and post monsoon period (Adhikary
509 et al., 2007). Similar behavior is seen this time for CO where the model misses the peak values
510 but reasonably captures CO concentration after mid-May. ~~Even though the model calculated~~
511 ~~values are lower in the present study, the model captures the synoptic variability fairly well for~~
512 ~~all the pollutants compared.~~ STEM model **CO** performance can be significantly improved via
513 better constraining ~~anthropogenic emissions inventory~~, emissions of open biomass burning **as**
514 **discussed in Section 3.3.** ~~(natural and anthropogenic) and improvements in meteorological output~~
515 ~~from WRF amongst many other uncertainties inherent in regional chemical transport model.~~ This
516 activity is beyond the scope of this current paper although the improvements are underway for all
517 these sectors.

518 **3.2.3 Diurnal variations of air pollutants and boundary layer height**

519 In the emission source region, diurnal variations of primary pollutants provide information about
520 the time dependent emission activities (Kumar et al., 2016b). **Figure 8** shows the diurnal
521 variation of hourly averaged concentrations of ~~various~~ measured pollutants during the sampling
522 period. Primary pollutants like **BC, PM and CO** showed typical characteristics of an urban
523 environment, i.e., diurnal variation with a morning and an evening peak. However, Lumbini data
524 shows higher concentrations in the evenings compared to morning hours. Elevated
525 concentrations can be linked to morning and evening cooking hours for BC and CO where
526 emission inventory show that residential sector has significant contribution. However,
527 explanation for elevated evening concentration compared to morning needs further investigation.
528 Increase in the depth of boundary layer, reduction in the traffic density on the roads, absence of
529 open biomass burning during mid-day and increasing wind speed often contribute to the
530 dispersion of pollutants resulting in lower concentration during afternoon. Diurnal variation of
531 wind direction (Supplementary information, Figure S1, ~~lower~~ **upper** panel) shows the dominance
532 of wind coming from south (mainly during the month of May and till mid-June). Morning and

533 evening period experienced the winds coming from the southeast direction while the winds were
534 predominantly from southwest direction during late afternoon. Increase in CO concentrations in
535 the evening hours might be due to transport of ~~higher levels~~ of CO ~~emissions~~ from source
536 regions upwind of Lumbini which along with the local emissions **which** gets trapped under lower
537 Planetary Boundary Layer (PBL) heights in evening and night time. Ozone concentration was
538 lowest in the morning before the sunrise and highest in late afternoon around 15:00 PM after
539 which concentrations started declining, exhibiting a typical characteristic of a polluted urban site.
540 Photo-dissociation of accumulated NO_x reservoirs (like HONO) provides sufficient NO
541 concentration leading to the titration of O₃ resulting in minimum O₃ just before sunrise (Kumar
542 et al., 2016b). The PBL height (in meters (m)) was obtained from the **WRF** model as
543 observations were not available. **Figure 9** shows the diurnal variation of the model derived PBL
544 height. The study period average PBL height over Lumbini was ~ 910 m (ranging between 24.28
545 and 3807 m observed at 06:00 and 15:00 h respectively). As the pre-monsoon month advances,
546 PBL height also increased. The monthly average PBL height was 799 m, 956 m and 1014 m
547 respectively during the month of April, May and (1st-15th) June. ~~Over the IGP region, PBL height~~
548 ~~is deeper during the pre monsoon compared to monsoon (Patil et al., 2014), post monsoon~~
549 ~~(Hegde et al., 2009) and winter (Badarinath et al., 2009) seasons.~~ The fluctuations of **modeled**
550 PBL height correspond well with the diurnal variation of **observed** the pollutants like BC, CO
551 and PM with the period of lower boundary height experiencing higher pollution concentration.

552 **3.3 Influence of forest fires on Lumbini air quality**

553 **3.3.1 Identification of forest fire influence over large scale using in-situ observations** 554 **satellite and model data**

555 Forest fires and **agricultural** biomass burning (mostly agro-residue burning in large scale) are
556 common over the South Asia and the IGP region during pre-monsoon season. North Indo-
557 Gangetic region is characterized by fires even during the monsoon and post-monsoon season
558 (Kumar et al., 2016b; Putero et al., 2014). These activities influence air quality not only over
559 nearby regions but also get transported towards high elevation pristine environments like **Mt.**
560 Everest (Putero et al., 2014) and Tibet (Cong et al., 2015a; 2015b). So, one of the main
561 objectives of this study was to identify the influence of open burning on Lumbini air quality.
562 Average wind speed during the whole measurement period was 2.4 m s⁻¹. Based on this data,

563 open fire counts within the grid size of 200×200 km centering over Lumbini was used for this
564 analysis assuming that the emissions will take a maximum period of one day to reach our
565 monitoring site. Forest fire counts were obtained from MODIS satellite data product called
566 Global Monthly Fire Location Products- (MCD14ML). More on this **product** has already been
567 described by Putero et al. (2014). **Figure 10** shows the daily average ~~in-situ CO, BC~~ $\Delta BC/\Delta CO$
568 **ratio**, aerosol absorption Ångstrom exponent (AAE) which is derived from Aethalometer data
569 and daily open fire count within the specified grid. The green box in the figure is used to show
570 two ~~outstanding~~ **peak** events (**presented earlier in Fig. 6**) with the elevated BC and CO
571 concentrations observed during the monitoring period. The first peak was observed during 7-9
572 April and second peak during 3-4 May, 2013. Two pollutants having biomass burning as the
573 potential primary source: BC and CO were taken in consideration. AAE values higher during
574 these two events (~ 1.6) are also an indication of presence of BC of biomass burning origin.
575 ~~Ground based TSP sampling also showed higher concentration of biomass burning tracer~~
576 ~~(potassium or K^+) in Lumbini during the pre-monsoon season comparing to other seasons of the~~
577 ~~year (L. Tripathee, personal communication).~~ **The chemical composition of TSP filter samples**
578 **collected at Lumbini also showed higher concentration of Levoglucosan, a biomass burning**
579 **tracer in Lumbini during the pre-monsoon season as compared to other seasons of the year (Wan**
580 **et al., 2016, Manuscript under review for ACPD). Wan et al. (2016) also reported that the higher**
581 **correlation between K^+ with tracers of dust (Ca^{2+} and Mg^{2+}) indicated that dust is the main**
582 **source of potassium in Lumbini.**

583 **Contrary to** ~~But,~~ to our expectation, we could not observe any significant influence of forest fire
584 within the specified grid **of 200x200 km** (or the influence of local forest fire on the air quality
585 over Lumbini was not observed). Therefore, a wider area, covering South and Southeast Asian
586 regions, was selected for the forest fire count. **Figure 11** (A-B) shows the active fire hotspots
587 from MODIS, over the region, during the peak events which shows the first peak occurred due to
588 the forest fire over the eastern India region whereas the second peak was influenced by the forest
589 fire over western IGP region. Moreover, in order to strengthen our hypothesis, we have utilized
590 satellite data products for various gaseous pollutants like CO and NO₂ (Atmospheric Infrared
591 Sounder (AIRS) for CO and Ozone Monitoring Instrument (OMI) for NO₂ both obtained from
592 Giovanni platform). **Figure 11** (C-H) shows the daytime total column CO before, during and
593 after occurrence of two events (peaks) as stated earlier. Atmospheric Infrared Sounder (AIRS)

594 satellite with daily temporal resolution and $1^{\circ}\times 1^{\circ}$ spatial resolution have been utilized to
595 understand the CO concentration over the area. CO concentration over Lumbini during both of
596 the peaks confirmed the role of open fires on either sides of the IGP region for elevated
597 concentration of CO over Lumbini. To further strengthen our finding, the aid of wind rose plot of
598 local wind speed and direction was taken. **Figure 11** (I-J) represent the wind rose plot only for
599 these two events respectively. Wind rose plots also confirm the wind blowing from those two
600 forest fire regions affected the air quality in Lumbini region. **Figure11** (K) shows model biomass
601 CO peak coincident with observed CO. Although the magnitudes are **significantly** different, the
602 timing of the peaks is well captured by the model. **However, This we believe is due to the fact**
603 **that** satellite based open fire detection also has limitation as it does not capture numerous small
604 fires that are prevalent over south Asia which usually burn out before the next satellite overpass.
605 More research is needed to assess the influence of these small fires on regional air quality.

606 In a separate analysis (not shown here), elevated O_3 concentration during these two events were
607 also observed. Average O_3 concentration before, during and after the events were found to be
608 46.2 ± 20.3 ppbv, 53.5 ± 31.1 ppbv and 50.3 ± 20.9 ppbv respectively (Event-I) whereas it was
609 found to be 54.8 ± 23.8 ppbv, 56.7 ± 35 ppbv and 55.6 ± 13.4 ppbv respectively (Event-II).
610 Increased ozone concentrations during the high peak events have been analyzed using the
611 satellite NO_2 concentration over the region considering the role of NO_2 as precursor for ozone
612 formation. Daily total column NO_2 were obtained from OMI satellite (data available at the
613 Giovanni platform; <http://giovanni.gsfc.nasa.gov/giovanni/>) at the spatial resolution of
614 $0.25^{\circ}\times 0.25^{\circ}$. **Figure 12** shows the NO_2 column value before, during and after both events. Even
615 for the NO_2 , maximum concentrations were observed during these two special events.

616 **3.3.2 Identifying regional and local contribution**

617 **WRF-STEM model has been used to identify the anthropogenic emission source region**
618 **influencing the air quality over Lumbini. As previously explained, the model is able to capture**
619 **the observed CO concentration when intense open burning events were not present. An attempt**
620 **has been undertaken to identify the source region contribution, utilizing the WRF-STEM model**
621 **results, for the CO concentrations observed at Lumbini.** A recent study (Kulkarni et al., 2015)
622 has explored the source region contribution of various pollutants over the Central Asia using
623 **similar technique** ~~the same model~~. **Figure 13** (A) shows the average contribution from different

624 regions on CO concentration over Lumbini during the whole measurement period. Major share
625 of CO was from the Ganges valley (46%) followed by Nepal region (25%) and rest of Indian
626 region (~17.5%). Contribution from other South Asian countries like Bangladesh and Pakistan
627 were ~ 11% whereas China contributed for ~1% of the CO concentration in Lumbini. **Regarding**
628 **the monthly average contribution, the Ganges Valley and Nepal's contribution were almost equal**
629 **during the month of April (~34% and ~37% respectively) but increased for the Ganges Valley**
630 **region during the month of May (~44%) and got reduced for Nepal region (~25%) (Figure S6).**

631 **Figure 13 (B)** is the time series of percentage contribution to total CO concentration during
632 whole measurement period showing different air mass arriving at a 3 hourly intervals. During the
633 whole measurement period, majority of the CO reaching Lumbini were from the Ganges valley
634 **(mainly the states of Punjab, Haryana, Uttar Pradesh, Bihar and West Bengal)** region with the
635 contribution sometimes reaching up to ~80%. Other India (central, south, east and north) regions
636 also contributed significantly. Bangladesh's contribution in CO loading was seen only after mid-
637 April lasting for only about a week and after the first week of May. The contribution from
638 Bangladesh was sporadic comparing to other regions. Highest contribution from this Bangladesh
639 region was observed after the first week of June **with the arrival of monsoonal air mass**. Pakistan
640 also contributed for the CO loading significantly. Others region as mentioned in the figure
641 covered the regions like Afghanistan, Middle east, West Asia, East Asia, Africa and Bhutan.
642 Contributions from these regions were less than 5%. Contribution from China was not evident
643 till the first week of June where a specific air mass arrival shows contribution reaching up to
644 25% of total CO loading.

645 A sensitivity analysis was performed for emission uncertainty in the model grid containing
646 Lumbini. Lumbini and surrounding regions in the recent years has seen significant rise in urban
647 activities and industrial activity and related emissions which may not be accurately reflected in
648 the HTAPv2 emissions inventory. A month long simulation was carried out with emissions from
649 Lumbini and the surrounding four grids off and another simulation with Lumbini and
650 surrounding four grid's emissions ~~sealed~~ **increased by** 5 times the amount from HTAPv2
651 emissions inventory. The results are shown in **Figure 13 (C)** as percentage increase or decrease
652 compared to model results using the current HTAPv2 emissions inventory. The black line shows
653 concentration as 100% for the current HTAPv2 emissions inventory. Despite making Lumbini

654 and the surrounding grids emissions zero, model calculation shows pollutant concentration on
655 average is still about 78% of the original value indicating dominance of background and regional
656 sources compared to local source in the model. Increasing emissions 5 times for the Lumbini and
657 surrounding four grids only increases the concentration on average by 151%. Thus uncertainty in
658 emissions are not a local uncertainty for Lumbini rather for the whole region which needs to be
659 better understood for improving model performance against observations at Lumbini.

660 **3.4 — Contribution of aerosol composition to local air quality as identified by the model**

661 ~~The chemical composition of $PM_{2.5}$ obtained from the model is shown in Figure 13.~~
662 ~~Carbonaceous aerosols and sulfate pollutants contributed two-third fraction of the fine mode~~
663 ~~particulate matter ($PM_{2.5}$). Organic carbon (OC) was found as the main constituent of the $PM_{2.5}$~~
664 ~~contributing ~45% to $PM_{2.5}$. For Lumbini, the contribution of modeled BC to $PM_{2.5}$ was ~10%~~
665 ~~similar to the observed (9.2%) fraction of BC to $PM_{2.5}$. Recent study conducted over nearby IGP~~
666 ~~site, Kanpur (Ram and Sarin, 2011) found the average share of OC and EC in $PM_{2.5}$ to be ~45%~~
667 ~~and ~5% respectively which is close to the values obtained by our model based calculation.~~
668 ~~Natural aerosols mainly wind blown mineral dust was ~25% of the fine mode PM in Lumbini.~~
669 ~~Highest loading of dust is observed during the late dry period to early monsoon season in South~~
670 ~~Asian region (Adhikary et al., 2007). Sulfate contributed for ~20% share of the $PM_{2.5}$ over~~
671 ~~Lumbini. Although the post monsoon season observed highest concentration of sulfate in South~~
672 ~~Asian region, elevated concentration are observed even during the April over Ganges Valley~~
673 ~~(Adhikary et al., 2007). As expected, very minimal contribution from sea salts (less than 1%)~~
674 ~~was observed at Lumbini.~~

675 **3.5 Does fossil fuel or biomass influence the Lumbini air?**

676 The aerosol spectral absorption is used to gain insight into nature and potential source of black
677 carbon. This method enables to analyze the contributions of fossil fuel combustion and biomass
678 burning contributions to the observed BC concentration (Kirchstetter et al., 2004). Besides BC,
679 other light absorbing (in the UV region) aerosols are also produced in course of combustion,
680 collectively termed as organic aerosols (often also called brown carbon or BrC) (Andreae and
681 Gelencsér, 2006). Figure 14 shows the comparison of normalized light absorption as function of
682 the wavelength for BC observed at Lumbini during cooking and non-cooking hours. Our results

683 are compared with the published data of Kirchstetter et al. (2004) and that observed over a
684 village center site of Project Surya in the IGP (Praveen et al., 2012) (figure not shown). We
685 discuss light absorption data from two distinct times of the day. The main reason behind using
686 data during 07:00-08:00 h and 16:00-17:00 h is these periods represent highest and lowest
687 ambient concentration (Fig. 8). Also these period represent cooking and non-cooking or high and
688 low vehicular movement hours (Praveen et al., 2012). To understand the influence of biomass
689 and fossil fuel we plotted normalized aerosol absorption at 700 nm wavelength for complete
690 aethalometer measured wavelengths in Fig. 14. Kirchstetter et al. (2004) reported OC absorption
691 efficiency at 700 nm to be zero. Thus we normalized measured absorption spectrum by 700 nm
692 wavelength absorption. Since aethalometer does not provide 700 nm wavelength absorption
693 values, we used methodology followed by Praveen et al. (2012). Our results show that the
694 normalized absorption for biomass burning aerosol is ~3 times higher at 370 nm compared to
695 that at 700 nm whereas fossil fuel absorption is about 2.6 times higher at the same wavelength.
696 The normalized curve obtained during both cooking and non-cooking period lies in between the
697 standard curve of Kirchstetter et al. (2004). ~~The curve during the prime cooking time is much
698 close to the biomass curve of published data (including that during the cooking period over the
699 village center site of Project Surya) whereas that during non-cooking time (afternoon period) is
700 inclined towards the fossil fuel curve.~~ As shown in Fig. 13, the curve obtained for the prime
701 cooking time is closer towards the published curve on biomass burning whereas that obtained
702 during the non-cooking time is closer towards the published fossil fuel curve. Similar result was
703 also observed over the Project Surya village in the IGP region (Praveen et al., 2012; Rehman et
704 al., 2011). This clearly indicates there is contribution of both sources: biomass as well as fossil
705 fuel on the observed BC concentration over Lumbini.

706 In order to identify fractional contribution of biomass burning and fossil fuel combustion to
707 observed BC aerosol, we adopted the method described by Sandradewi et al. (2008). Wavelength
708 dependence of aerosol absorption coefficient (b_{abs}) is proportional to $\lambda^{-\alpha}$ where λ is the
709 wavelength and α is the absorption Ångstrom exponent. The α values ranges from 0.9-2.2 for
710 fresh wood smoke aerosol (Day et al., 2006) and between 0.8-1.1 for traffic or diesel soot
711 (references in Sandradewi et al. (2008)). We have taken α value of 1.86 for biomass burning and
712 1.1 for fossil fuel burning as suggested by previous literature (Sandradewi et al., 2008). Figure
713 15 shows diurnal variation of the biomass burning BC. Minimum contribution of biomass

714 burning to total BC concentration was observed during 04:00-06:00 local time (only about 30%
715 of the total BC). As the cooking activities start in morning, the contribution of biomass BC starts
716 to increase and reaches about 50%. Similar pattern was repeated during evening cooking hours.
717 Only during these two cooking periods, fossil fuel fraction BC was lower. Otherwise it remained
718 significantly higher than biomass burning BC throughout the day. On average, ~40% of BC was
719 from biomass burning whereas remaining 60% was contributed by fossil fuel combustion during
720 our measurement period. Interestingly, this is the opposite of the contributions that were
721 concluded by Lawrence and Lelieveld (2010). Lawrence and Lelieveld (2010) concluded that
722 ~60% BC from biomass versus ~40% fossil fuel, based on a review of numerous previous
723 studies to be likely for the outflow from Southern Asia during the winter monsoon. When we
724 compared observed Ångstrom exponent with Praveen et al. (2012), we noticed that Lumbini
725 values were lower than Project Surya Village center site. This implies Surya village center had
726 higher biomass fraction, also it was observed absorption Ångstrom exponent exceeded 1.86
727 during cooking hours which indicates 100% biomass contribution. The difference is attributed to
728 the fact that Lumbini sampling site is not a residential site like Surya village which can capture
729 cooking influence efficiently. Further Lumbini sampling site is surrounded by commercial
730 activities such as a local bus park, hotels, office buildings and industries and brick kilns slightly
731 further away. Although the reason for this difference is not clear, it is an indication of the
732 important role of diesel and coal emissions in the Lumbini and upwind regions.

733 4. Conclusions

734 Our measurements, a first for the Lumbini area, have shown very high pollution concentration at
735 Lumbini. Black carbon (BC), carbon monoxide (CO), ozone (O₃) and particulate matter (PM₁₀,
736 PM_{2.5} and PM₁) were measured during the pre-monsoon of 2013 as a regional site of the *SusKat-*
737 *ABC campaign*. Average pollutant concentrations during the monitoring period were found to be:
738 BC: $4.9 \pm 3.8 \mu\text{g m}^{-3}$; CO: $344.1 \pm 160.3 \text{ ppbv}$; O₃: $46.6 \pm 20.3 \text{ ppbv}$; PM₁₀: $128.8 \pm 91.9 \mu\text{g m}^{-3}$
739 PM_{2.5}: $53.14 \pm 35.1 \mu\text{g m}^{-3}$ and **PM₁: $36.6 \pm 25.7 \mu\text{g m}^{-3}$** which is comparable with other urban sites
740 like Kanpur and Delhi **in the IGP region. However, our study finds higher fraction of coarse**
741 **mode PM in Lumbini as compared to other sites in the IGP region. In addition, $\Delta\text{BC}/\Delta\text{CO}$ ratio**
742 **obtained in Lumbini was within the range of emission from both domestic and transportation**
743 **sectors, indicating them as potential key sources of BC and CO, and likely most of PM₁ in**

744 **Lumbini**. The diurnal variation of the pollutants is similar to that of any urban location, with
745 peaks during morning and evening. However, our results show higher evening concentration
746 compared to morning concentration **values and needs further research to explain this behavior**.
747 During our measurement period, air quality in Lumbini was influenced by regional forest fires as
748 shown by **chemical transport** model and satellite data analysis. A regional chemical transport
749 model, WRF-STEM was used to interpret observations. Inter-comparison of WRF-STEM model
750 outputs with observations showed that the model underestimated the observed pollutant
751 concentrations by a factor of 1.5 to 5 **but was able to capture the temporal variability**.
752 ~~Nonetheless, WRF-STEM model was able to simulate the synoptic variability of observed~~
753 ~~pollutants~~. Model uncertainties are attributed mostly to uncertainties in meteorology and regional
754 emissions **as shown from sensitivity analysis with local emissions**. Region-tagged CO as air-
755 mass tracers are employed in **WRF-STEM model** to understand the **anthropogenic emission**
756 source region influencing Lumbini. Our analysis shows that the adjacent regions; mostly the
757 Ganges valley, other parts of India and Nepal accounted for the highest contribution to pollutant
758 concentration in the Lumbini. ~~Anthropogenic pollutants in PM_{2.5} were dominant, with OC and~~
759 ~~BC contributing ~45% and ~10%, respectively while sulfate aerosol contributed to 20%,~~
760 ~~whereas natural pollutants like mineral dust contributed ~25%~~. The normalized light absorption
761 curve clearly indicated the contribution to BC in Lumbini from both sources: biomass as well as
762 fossil fuel. On average, ~40% BC was found to be from the biomass burning and ~60% from
763 fossil fuel burning.

764 Various improvements and extensions would be possible in future studies. More reliable
765 functioning of the AWS (temperature and RH sensor, rain gauge) would have allowed more in-
766 depth analysis of the relationship between meteorological parameters and pollutants
767 concentration. Continuous measurements of air pollutants throughout the year would allow for
768 annual and seasonal variation study. Improvements in the model are much needed in its ability to
769 simulate observed meteorology. Significant uncertainty lies with regional emissions inventory
770 **developed at national and continental scale versus local bottoms up inventory** and **pollutant**
771 emissions from **small scale** open burning **not captured by satellites**.

772 There is a clear need for setting up of a continuous air quality monitoring station at Lumbini
773 (UNESCO World Heritage Site) and the surrounding regions for long-term air quality

774 monitoring. ~~In order to fully safeguard the valuable world heritage properties as well as public~~
775 ~~health and agro-ecosystems in the region from impacts of air pollution, development activities~~
776 ~~within the Kenzo Tange Master Plan Area and Lumbini Protected Zone (LPZ) need to go~~
777 ~~through a rigorous environmental impact assessment (EIA) and heritage impact assessment~~
778 ~~(HIA) in accordance with the decisions of the UNESCO World Heritage Committee.~~

779 **Data availability**

780 The data used for this manuscript can be obtained by sending an email to the corresponding
781 authors and/or to IASS (Maheswar.Rupakheti@iass.potsdam.de) and/or to ICIMOD
782 (arnico.panday@icimod.org). Modeling codes data can be obtained from B. Adhikary
783 (Bhupesh.adhikary@icimod.org).

784 **Authors' contributions**

785 M.R. and M.L. conceived the **Lumbini portion of the SusKat** experiment. M.R. and A.K.P.
786 coordinated the **Lumbini** field campaign. D.R. and K.S.M conducted the field observations **at**
787 **Lumbini**. B.A. designed and ran the WRF-STEM model. P.S.P., B.A. and D.R. finalized the
788 manuscript composition. D.R., P.S.P, B.A., M.R. and S.K. conducted the data analysis. D.R. **and**
789 **B.A.** prepared the manuscript with inputs from all coauthors.

790

791 **Acknowledgements**

792 This study was partly supported by the Institute for Advanced Sustainability Studies (IASS),
793 Germany, the International Centre for Integrated Mountain Development (ICIMOD), and the
794 National Natural Science Foundation of China (41121001, 41225002), and the Strategic Priority
795 Research Program (B) of the Chinese Academy of Sciences (XDB03030504). Dipesh Rupakheti
796 is supported by CAS-TWAS President's Fellowship for International PhD Students. **The IASS is**
797 **grateful for its funding from the German Federal Ministry for Education and Research (BMBF)**
798 **and the Brandenburg Ministry for Science, Research and Culture (MWFK).** ICIMOD authors
799 would like to acknowledge that this study was partially supported by core funds of ICIMOD
800 contributed by the governments of Afghanistan, Australia, Austria, Bangladesh, Bhutan, China,
801 India, Myanmar, Nepal, Norway, Pakistan, Switzerland, and the United Kingdom. The views and

802 interpretations in this publication are those of the authors and are not necessarily attributable to
803 the institutions they are associated with. We thank B. Kathayat, B.R. Bhatta, and Venerable
804 Vivekananda and his colleagues (Panditarama Lumbini International Vipassana Meditation
805 Center) for providing logistical support which was vital in setting up and running the site. We
806 also thank C. Cüppers and M. Pahlke of the Lumbini International Research Institute (LIRI) for
807 providing the space and power to run the instruments at the LIRI premises. Satellite data providers
808 (MODIS, AIRS, OMI) are also equally acknowledged.

809

810 **References**

- 811 Adhikary, B., Carmichael, G. R., Tang, Y., Leung, L. R., Qian, Y., Schauer, J. J., Stone, E. A.,
812 Ramanathan, V., and Ramana, M. V.: Characterization of the seasonal cycle of south Asian aerosols:
813 A regional-scale modeling analysis, *J. Geophys. Res.*, 112, D22S22, doi: 10.1029/2006jd008143,
814 2007.
- 815 Andreae, M. O., and Gelencsér, A.: Black carbon or brown carbon? The nature of light-absorbing
816 carbonaceous aerosols, *Atmos. Chem. Phys.*, 6, 3131-3148, doi: 10.5194/acp-6-3131-2006, 2006.
- 817 ~~Badarinath, K., Sharma, A. R., Kharol, S. K., and Prasad, V. K.: Variations in CO, O₃ and black carbon
818 aerosol mass concentrations associated with planetary boundary layer (PBL) over tropical urban
819 environment in India, *J. Atmos. Chem.*, 62, 73-86, doi: 10.1007/s10874-009-9137-2, 2009.~~
- 820 Baedecker, P. A., Reddy, M. M., Reimann, K. J., and Sciammarella, C. A.: Effects of acidic deposition on
821 the erosion of carbonate stone — experimental results from the U.S. National Acid Precipitation
822 Assessment Program (NAPAP), *Atmos. Environ.*, 26, 147-158, doi: 10.1016/0957-1272(92)90018-N,
823 1992.
- 824 Bergin, M. H., Tripathi, S. N., Jai Devi, J., Gupta, T., McKenzie, M., Rana, K., Shafer, M. M., Villalobos,
825 A. M., and Schauer, J. J.: The Discoloration of the Taj Mahal due to Particulate Carbon and Dust
826 Deposition, *Environ. Sci. Technol.*, 49, 808-812, doi: 10.1021/es504005q, 2015.
- 827 Bisht, D. S., Dumka, U. C., Kaskaoutis, D. G., Pipal, A. S., Srivastava, A. K., Soni, V. K., Attri, S. D.,
828 Sateesh, M., and Tiwari, S.: Carbonaceous aerosols and pollutants over Delhi urban environment:
829 Temporal evolution, source apportionment and radiative forcing, *Sci. Total Environ.*, 521-522C, 431-
830 445, doi: 10.1016/j.scitotenv.2015.03.083, 2015.
- 831 Bonasoni, P., Laj, P., Marinoni, A., Sprenger, M., Angelini, F., Arduini, J., Bonafè, U., Calzolari, F.,
832 Colombo, T., Decesari, S., Di Biagio, C., di Sarra, A. G., Evangelisti, F., Duchi, R., Facchini, M. C.,
833 Fuzzi, S., Gobbi, G. P., Maione, M., Panday, A., Roccato, F., Sellegri, K., Venzac, H., Verza, G. P.,
834 Villani, P., Vuillermoz, E., and Cristofanelli, P.: Atmospheric Brown Clouds in the Himalayas: first
835 two years of continuous observations at the Nepal Climate Observatory-Pyramid (5079 m), *Atmos.*
836 *Chem. Phys.*, 10, 7515-7531, doi: 10.5194/acp-10-7515-2010, 2010.
- 837 Brimblecombe, P.: The effects of air pollution on the built environment, Imperial College Press, London,
838 2003.
- 839 Burney, J., and Ramanathan, V.: Recent climate and air pollution impacts on Indian agriculture, *Proc.*
840 *Natl. Acad. Sci. USA*, 111, 16319-16324, doi: 10.1073/pnas.1317275111, 2014.
- 841 **Cao, J.-J., Zhu, C.-S., Chow, J. C., Watson, J. G., Han, Y.-M., Wang, G.-h., Shen, Z.-x., and An, Z.-S.:**
842 **Black carbon relationships with emissions and meteorology in Xi'an, China, *Atmospheric Research*,**
843 **94, 194-202, <http://dx.doi.org/10.1016/j.atmosres.2009.05.009>, 2009.**
- 844 Cong, Z., Kang, S., Kawamura, K., Liu, B., Wan, X., Wang, Z., Gao, S., and Fu, P.: Carbonaceous
845 aerosols on the south edge of the Tibetan Plateau: concentrations, seasonality and sources, *Atmos.*
846 *Chem. Phys.*, 15, 1573-1584, doi: 10.5194/acp-15-1573-2015, 2015a.
- 847 Cong, Z., Kawamura, K., Kang, S., and Fu, P.: Penetration of biomass-burning emissions from South
848 Asia through the Himalayas: new insights from atmospheric organic acids, *Sci. Rep.*, 5, doi:
849 10.1038/srep09580, 2015b.
- 850 Cristofanelli, P., Bracci, A., Sprenger, M., Marinoni, A., Bonafè, U., Calzolari, F., Duchi, R., Laj, P.,
851 Pichon, J. M., Roccato, F., Venzac, H., Vuillermoz, E., and Bonasoni, P.: Tropospheric ozone
852 variations at the Nepal Climate Observatory-Pyramid (Himalayas, 5079 m a.s.l.) and influence of
853 deep stratospheric intrusion events, *Atmos. Chem. Phys.*, 10, 6537-6549, doi: 10.5194/acp-10-6537-
854 2010, 2010.
- 855 Das, S. K., and Jayaraman, A.: Role of black carbon in aerosol properties and radiative forcing over
856 western India during premonsoon period, *Atmos. Res.*, 102, 320-334, doi:
857 10.1016/j.atmosres.2011.08.003, 2011.

858 Day, D., Hand, J., Carrico, C., Engling, G., and Malm, W.: Humidification factors from laboratory studies
859 of fresh smoke from biomass fuels, *J. Geophys. Res.*, 111, D22202, doi: 10.1029/2006JD007221,
860 2006.

861 Dickerson, R. R., Andreae, M. O., Campos, T., Mayol-Bracero, O. L., Neusuess, C., and Streets, D. G.:
862 Analysis of black carbon and carbon monoxide observed over the Indian Ocean: Implications for
863 emissions and photochemistry, *Journal of Geophysical Research: Atmospheres*, 107, INX2 16-11-
864 INX12 16-11, 10.1029/2001JD000501, 2002.

865 Duchi, R., Cristofanelli, P., Marinoni, A., Laj, P., Marcq, S., Villani, P., Sellegri, K., Angelini, F.,
866 Calzolari, F., Gobbi, G. P., Verza, G. P., Vuillermoz, E., Sapkota, A., and Bonasoni, P.: Continuous
867 observations of synoptic-scale dust transport at the Nepal Climate Observatory-Pyramid (5079 m
868 a.s.l.) in the Himalayas, *Atmos. Chem. Phys. Discuss.*, 11, 4229-4261, doi: 10.5194/acpd-11-4229-
869 2011, 2011.

870 Forouzanfar, M. H., Alexander, L., Anderson, H. R., Bachman, V. F., Biryukov, S., Brauer, M., Burnett,
871 R., Casey, D., Coates, M. M., and Cohen, A.: Global, regional, and national comparative risk
872 assessment of 79 behavioural, environmental and occupational, and metabolic risks or clusters of
873 risks in 188 countries, 1990–2013: a systematic analysis for the Global Burden of Disease Study
874 2013, *Lancet*, 386, 2287-2323, doi: 10.1016/S0140-6736(15)00128-2, 2015.

875 Ganguly, D., Jayaraman, A., Rajesh, T. A., and Gadhavi, H.: Wintertime aerosol properties during foggy
876 and nonfoggy days over urban center Delhi and their implications for shortwave radiative forcing, *J.*
877 *Geophys. Res.*, 111, D15217, doi: 10.1029/2005jd007029, 2006.

878 Gaur, A., Tripathi, S. N., Kanawade, V. P., Tare, V., and Shukla, S. P.: Four-year measurements of trace
879 gases (SO₂, NO_x, CO, and O₃) at an urban location, Kanpur, in Northern India, *J. Atmos. Chem.*, 71,
880 283-301, doi: 10.1007/s10874-014-9295-8, 2014.

881 Gauri, K. L., and Holdren, G.: Pollutant effects on stone monuments, *Environ. Sci. Technol.*, 15, 386-390,
882 doi: 10.1021/es00086a001, 1981.

883 Girach, I. A., Nair, V. S., Babu, S. S., and Nair, P. R.: Black carbon and carbon monoxide over Bay of
884 Bengal during W_ICARB: Source characteristics, *Atmospheric Environment*, 94, 508-517,
885 <http://dx.doi.org/10.1016/j.atmosenv.2014.05.054>, 2014.

886 Hegde, P., Pant, P., and Bhavani Kumar, Y.: ~~An integrated analysis of lidar observations in association
887 with optical properties of aerosols from a high altitude location in central Himalayas, *Atmos. Sci.*
888 *Lett.*, 10, 48-57, doi: 10.1002/asl.209, 2009.~~

889 Huang, X.-F., Sun, T.-L., Zeng, L.-W., Yu, G.-H., and Luan, S.-J.: Black carbon aerosol characterization
890 in a coastal city in South China using a single particle soot photometer, *Atmospheric Environment*,
891 51, 21-28, <http://dx.doi.org/10.1016/j.atmosenv.2012.01.056>, 2012.

892 IPCC: Climate Change 2013: The Physical Science Basis. Contribution of Working Group I to the Fifth
893 Assessment Report of the Intergovernmental Panel on Climate Change [Stocker, T.F., D. Qin, G.-K.
894 Plattner, M. Tignor, S.K. Allen, J. Boschung, A. Nauels, Y. Xia, V. Bex and P.M. Midgley (eds.)]. ,
895 2013.

896 Joshi, H., Naja, M., Singh, K., Kumar, R., Bhardwaj, P., Babu, S. S., Satheesh, S., Moorthy, K. K., and
897 Chandola, H.: Investigations of aerosol black carbon from a semi-urban site in the Indo-Gangetic
898 Plain region, *Atmos. Environ.*, 125, 346-359, doi: 10.1016/j.atmosenv.2015.04.007, 2016.

899 Kirchstetter, T. W., Novakov, T., and Hobbs, P. V.: Evidence that the spectral dependence of light
900 absorption by aerosols is affected by organic carbon, *J. Geophys. Res.*, 109, D21208,
901 doi:10.1029/2004JD004999, 2004.

902 Kulkarni, S., Sobhani, N., Miller-Schulze, J. P., Shafer, M. M., Schauer, J. J., Solomon, P. A., Saide, P.
903 E., Spak, S. N., Cheng, Y. F., Denier van der Gon, H. A. C., Lu, Z., Streets, D. G., Janssens-
904 Maenhout, G., Wiedinmyer, C., Lantz, J., Artamonova, M., Chen, B., Imashev, S., Sverdlik, L.,
905 Deminter, J. T., Adhikary, B., D'Allura, A., Wei, C., and Carmichael, G. R.: Source sector and region
906 contributions to BC and PM_{2.5} in Central Asia, *Atmos. Chem. Phys.*, 15, 1683-1705, doi:
907 10.5194/acp-15-1683-2015, 2015.

908 Kumar, B., Chakraborty, A., Tripathi, S. N., and Bhattu, D.: Highly time resolved chemical
909 characterization of submicron organic aerosols at a polluted urban location, *Environmental Science:
910 Processes & Impacts*, 18, 1285-1296, 10.1039/C6EM00392C, 2016a.

911 Kumar, M., Tiwari, S., Murari, V., Singh, A. K., and Banerjee, T.: Wintertime characteristics of aerosols
912 at middle Indo-Gangetic Plain: Impacts of regional meteorology and long range transport, *Atmos.
913 Environ.*, 104, 162-175, 10.1016/j.atmosenv.2015.01.014, 2015.

914 Kumar, V., Sarkar, C., and Sinha, V.: Influence of post harvest crop residue fires on surface ozone mixing
915 ratios in the NW IGP analyzed using two years of continuous in-situ trace gas measurements, *J.
916 Geophys. Res. Atmos.*, 121, 3619–3633, doi: 10.1002/2015JD024308, 2016b.

917 Lawrence, M. G., and Lelieveld, J.: Atmospheric pollutant outflow from southern Asia: a review, *Atmos.
918 Chem. Phys.*, 10, 11017-11096, doi: 10.5194/acp-10-11017-2010, 2010.

919 Lüthi, Z. L., Škerlak, B., Kim, S. W., Lauer, A., Mues, A., Rupakheti, M., and Kang, S.: Atmospheric
920 brown clouds reach the Tibetan Plateau by crossing the Himalayas, *Atmos. Chem. Phys.*, 15, 6007-
921 6021, doi: 10.5194/acp-15-6007-2015, 2015.

922 Marinoni, A., Cristofanelli, P., Laj, P., Duchi, R., Putero, D., Calzolari, F., Landi, T. C., Vuillermoz, E.,
923 Maione, M., and Bonasoni, P.: High black carbon and ozone concentrations during pollution transport
924 in the Himalayas: Five years of continuous observations at NCO-P global GAW station, *J. Environ.
925 Sci.-China*, 25, 1618-1625, doi: 10.1016/s1001-0742(12)60242-3, 2013.

926 Misra, A., Gaur, A., Bhattu, D., Ghosh, S., Dwivedi, A. K., Dalai, R., Paul, D., Gupta, T., Tare, V.,
927 Mishra, S. K., Singh, S., and Tripathi, S. N.: An overview of the physico-chemical characteristics of
928 dust at Kanpur in the central Indo-Gangetic basin, *Atmospheric Environment*, 97, 386-396,
929 <http://dx.doi.org/10.1016/j.atmosenv.2014.08.043>, 2014.

930 Mohnen, V. A., Goldstein, W., and Wang, W. C.: Tropospheric Ozone and Climate Change, *Air & Waste*,
931 43, 1332-1334, doi: 10.1080/1073161x.1993.10467207, 1993.

932 Naja, M., Lal, S., and Chand, D.: Diurnal and seasonal variabilities in surface ozone at a high altitude site
933 Mt Abu (24.6° N, 72.7° E, 1680m asl) in India, *Atmos. Environ.*, 37, 4205-4215, doi: 10.1016/S1352-
934 2310(03)00565-X, 2003.

935 Naja, M., Mallik, C., Sarangi, T., Sheel, V., and Lal, S.: SO₂ measurements at a high altitude site in the
936 central Himalayas: Role of regional transport, *Atmos. Environ.*, 99, 392-402, doi:
937 10.1016/j.atmosenv.2014.08.031, 2014.

938 Pan, X. L., Kanaya, Y., Wang, Z. F., Liu, Y., Pochanart, P., Akimoto, H., Sun, Y. L., Dong, H. B., Li, J.,
939 Irie, H., and Takigawa, M.: Correlation of black carbon aerosol and carbon monoxide in the high-
940 altitude environment of Mt. Huang in Eastern China, *Atmos. Chem. Phys.*, 11, 9735-9747, doi:
941 10.5194/acp-11-9735-2011, 2011.

942 Panday, A. K., and Prinn, R. G.: Diurnal cycle of air pollution in the Kathmandu Valley, Nepal:
943 Observations, *J. Geophys. Res.*, 114, D09305, doi: 10.1029/2008jd009777, 2009.

944 Pathak, B., Bhuyan, P. K., Biswas, J., and Takemura, T.: Long term climatology of particulate matter and
945 associated microphysical and optical properties over Dibrugarh, North-East India and inter-
946 comparison with SPRINTARS simulations, *Atmospheric Environment*, 69, 334-344,
947 <http://dx.doi.org/10.1016/j.atmosenv.2012.12.032>, 2013.

948 Patil, M., Patil, S., Waghmare, R., and Dharmaraj, T.: Planetary Boundary Layer and aerosol interactions
949 over the Indian sub-continent, *J. Atmos. Sol.-Terr. Phy.*, 112, 38-42, doi: 10.1016/j.jastp.2014.02.007,
950 2014.

951 Praveen, P. S., Ahmed, T., Kar, A., Rehman, I. H., and Ramanathan, V.: Link between local scale BC
952 emissions in the Indo-Gangetic Plains and large scale atmospheric solar absorption, *Atmos. Chem.
953 Phys.*, 12, 1173-1187, doi: 10.5194/acp-12-1173-2012, 2012.

954 Putero, D., Landi, T., Cristofanelli, P., Marinoni, A., Laj, P., Duchi, R., Calzolari, F., Verza, G., and
955 Bonasoni, P.: Influence of open vegetation fires on black carbon and ozone variability in the southern
956 Himalayas (NCO-P, 5079 m asl), *Environ. Pollut.*, 184, 597-604, doi: 10.1016/j.envpol.2013.09.035,
957 2014.

958 Putero, D., Cristofanelli, P., Marinoni, A., Adhikary, B., Duchì, R., Shrestha, S. D., Verza, G. P., Landi,
959 T. C., Calzolari, F., Busetto, M., Agrillo, G., Biancofiore, F., Di Carlo, P., Panday, A. K., Rupakheti,
960 M., and Bonasoni, P.: Seasonal variation of ozone and black carbon observed at Paknajol, an urban
961 site in the Kathmandu Valley, Nepal, *Atmos. Chem. Phys. Discuss.*, 15, 22527-22566, 10.5194/acpd-
962 15-22527-2015, 2015a.

963 ~~Putero, D., Cristofanelli, P., Marinoni, A., Adhikary, B., Duchì, R., Shrestha, S. D., Verza, G. P., Landi,
964 T. C., Calzolari, F., Busetto, M., Agrillo, G., Biancofiore, F., Di Carlo, P., Panday, A. K., Rupakheti,
965 M., and Bonasoni, P.: Seasonal variation of ozone and black carbon observed at Paknajol, an urban
966 site in the Kathmandu Valley, Nepal, *Atmos. Chem. Phys.*, 15, 13957-13971, doi: 10.5194/acp-15-
967 13957-2015, 2015b.~~

968 Ram, K., Sarin, M., and Tripathi, S.: A 1 year record of carbonaceous aerosols from an urban site in the
969 Indo-Gangetic Plain: Characterization, sources, and temporal variability, *J. Geophys. Res.*, 115,
970 D24313, doi: 10.1029/2010JD014188, 2010.

971 ~~Ram, K., and Sarin, M. M.: Day night variability of EC, OC, WSOC and inorganic ions in urban
972 environment of Indo-Gangetic Plain: Implications to secondary aerosol formation, *Atmos. Environ.*,
973 45, 460-468, doi: 10.1016/j.atmosenv.2010.09.055, 2011.~~

974 **Ramachandran, S., and Rajesh, T. A.: Black carbon aerosol mass concentrations over Ahmedabad, an
975 urban location in western India: Comparison with urban sites in Asia, Europe, Canada, and the United
976 States, *Journal of Geophysical Research: Atmospheres*, 112, n/a-n/a, 10.1029/2006JD007488, 2007.**

977 Ramanathan, V., Li, F., Ramana, M., Praveen, P., Kim, D., Corrigan, C., Nguyen, H., Stone, E. A.,
978 Schauer, J. J., and Carmichael, G.: Atmospheric brown clouds: Hemispherical and regional variations
979 in long-range transport, absorption, and radiative forcing, *J. Geophys. Res.*, 112, D22S21, doi:
980 10.1029/2006JD008124, 2007.

981 Ramanathan, V., and Carmichael, G.: Global and regional climate changes due to black carbon, *Nat.*
982 *Geosci.*, 1, 221-227, 2008.

983 Rastogi, N., Singh, A., Sarin, M. M., and Singh, D.: Temporal variability of primary and secondary
984 aerosols over northern India: Impact of biomass burning emissions, *Atmos. Environ.*, 125, 396-403,
985 doi: 10.1016/j.atmosenv.2015.06.010, 2016.

986 Rehman, I. H., Ahmed, T., Praveen, P. S., Kar, A., and Ramanathan, V.: Black carbon emissions from
987 biomass and fossil fuels in rural India, *Atmospheric Chemistry and Physics*, 11, 7289-7299,
988 10.5194/acp-11-7289-2011, 2011.

989 Safai, P. D., Kewat, S., Pandithurai, G., Praveen, P. S., Ali, K., Tiwari, S., Rao, P. S. P., Budhawant, K.
990 B., Saha, S. K., and Devara, P. C. S.: Aerosol characteristics during winter fog at Agra, North India, *J.*
991 *Atmos. Chem.*, 61, 101-118, doi: 10.1007/s10874-009-9127-4, 2009.

992 Sandradewi, J., Prévôt, A. S. H., Szidat, S., Perron, N., Alfarra, M. R., Lanz, V. A., Weingartner, E., and
993 Baltensperger, U.: Using Aerosol Light Absorption Measurements for the Quantitative Determination
994 of Wood Burning and Traffic Emission Contributions to Particulate Matter, *Environ. Sci. Technol.*,
995 42, 3316-3323, doi: 10.1021/es702253m, 2008.

996 Sarkar, C., Kumar, V., and Sinha, V.: Massive emissions of carcinogenic benzenoids from paddy residue
997 burning in north India, *Curr. Sci. India*, 104, 1703-1709, 2013.

998 Schmid, O., Artaxo, P., Arnott, W. P., Chand, D., Gatti, L. V., Frank, G. P., Hoffer, A., Schnaiter, M., and
999 Andreae, M. O.: Spectral light absorption by ambient aerosols influenced by biomass burning in the
1000 Amazon Basin. I: Comparison and field calibration of absorption measurement techniques, *Atmos.*
1001 *Chem. Phys.*, 6, 3443-3462, doi: 10.5194/acp-6-3443-2006, 2006.

1002 Sharma, R. K., Bhattarai, B. K., Sapkota, B. K., Gewali, M. B., and Kjeldstad, B.: Black carbon aerosols
1003 variation in Kathmandu valley, Nepal, *Atmos. Environ.*, 63, 282-288, doi:
1004 10.1016/j.atmosenv.2012.09.023, 2012.

1005 **Sharma, S., Brook, J. R., Cachier, H., Chow, J., Gaudenzi, A., and Lu, G.: Light absorption and thermal
1006 measurements of black carbon in different regions of Canada, *Journal of Geophysical Research:*
1007 *Atmospheres*, 107, AAC 11-11-AAC 11-11, 10.1029/2002JD002496, 2002.**

1008 Shindell, D.: Integrated Assessment of Black Carbon and Tropospheric Ozone: Summary for Decision
1009 Makers, United Nations Environment Programme, 2011.

1010 Sinha, V., Kumar, V., and Sarkar, C.: Chemical composition of pre-monsoon air in the Indo-Gangetic
1011 Plain measured using a new air quality facility and PTR-MS: high surface ozone and strong influence
1012 of biomass burning, *Atmos. Chem. Phys.*, 14, 5921-5941, doi: 10.5194/acp-14-5921-2014, 2014.

1013 Skamarock, W., Klemp, J., Dudhia, J., Gill, D., and Barker, D.: A description of the Advanced Research
1014 WRF version 3, Technical Report NCAR/TN475+STR, National Center for Atmospheric Research
1015 Technical Note, Boulder, Colorado, 2008.

1016 Snider, G., Weagle, C. L., Murdymootoo, K. K., Ring, A., Ritchie, Y., Stone, E., Walsh, A., Akoshile, C.,
1017 Anh, N. X., Balasubramanian, R., Brook, J., Qonitan, F. D., Dong, J., Griffith, D., He, K., Holben, B.
1018 N., Kahn, R., Lagrosas, N., Lestari, P., Ma, Z., Misra, A., Norford, L. K., Quel, E. J., Salam, A.,
1019 Schichtel, B., Segev, L., Tripathi, S., Wang, C., Yu, C., Zhang, Q., Zhang, Y., Brauer, M., Cohen, A.,
1020 Gibson, M. D., Liu, Y., Martins, J. V., Rudich, Y., and Martin, R. V.: Variation in global chemical
1021 composition of PM_{2.5}: emerging results from SPARTAN, *Atmos. Chem. Phys.*, 16, 9629-9653,
1022 10.5194/acp-16-9629-2016, 2016.

1023 Srivastava, A. K., Tiwari, S., Devara, P. C. S., Bisht, D. S., Srivastava, M. K., Tripathi, S. N., Goloub, P.,
1024 and Holben, B. N.: Pre-monsoon aerosol characteristics over the Indo-Gangetic Basin: implications to
1025 climatic impact, *Ann. Geophys.*, 29, 789-804, doi: 10.5194/angeo-29-789-2011, 2011.

1026 Stevenson, D., Dentener, F., Schultz, M., Ellingsen, K., Van Noije, T., Wild, O., Zeng, G., Amann, M.,
1027 Atherton, C., and Bell, N.: Multimodel ensemble simulations of present-day and near-future
1028 tropospheric ozone, *J. Geophys. Res.*, 111, D08301, doi: 10.1029/2005JD006338, 2006.

1029 Tiwari, S., Srivastava, A. K., Bisht, D. S., Parmita, P., Srivastava, M. K., and Attri, S. D.: Diurnal and
1030 seasonal variations of black carbon and PM_{2.5} over New Delhi, India: Influence of meteorology,
1031 *Atmospheric Research*, 125-126, 50-62, 10.1016/j.atmosres.2013.01.011, 2013.

1032 Tiwari, S., Pital, A. S., Hopke, P. K., Bisht, D. S., Srivastava, A. K., Tiwari, S., Saxena, P. N., Khan, A.
1033 H., and Pervez, S.: Study of the carbonaceous aerosol and morphological analysis of fine particles
1034 along with their mixing state in Delhi, India: a case study, *Environmental science and pollution*
1035 *research international*, 10.1007/s11356-015-4272-6, 2015.

1036 Tiwari, S., Dumka, U. C., Kaskaoutis, D. G., Ram, K., Panicker, A. S., Srivastava, M. K., Tiwari, S.,
1037 Attri, S. D., Soni, V. K., and Pandey, A. K.: Aerosol chemical characterization and role of
1038 carbonaceous aerosol on radiative effect over Varanasi in central Indo-Gangetic Plain, *Atmospheric*
1039 *Environment*, 125, Part B, 437-449, <http://dx.doi.org/10.1016/j.atmosenv.2015.07.031>, 2016.

1040 Tiwari, S., Dumka, U. C., Gautam, A. S., Kaskaoutis, D. G., Srivastava, A. K., Bisht, D. S., Chakrabarty,
1041 R. K., Sumlin, B. J., and Solmon, F.: Assessment of PM_{2.5} and PM₁₀ over Guwahati in Brahmaputra
1042 River Valley: Temporal evolution, source apportionment and meteorological dependence,
1043 *Atmospheric Pollution Research*, 8, 13-28, <http://dx.doi.org/10.1016/j.apr.2016.07.008>, 2017.

1044 Trivedi, D. K., Ali, K., and Beig, G.: Impact of meteorological parameters on the development of fine and
1045 coarse particles over Delhi, *Science of The Total Environment*, 478, 175-183,
1046 <http://dx.doi.org/10.1016/j.scitotenv.2014.01.101>, 2014.

1047 Verma, R. L., Sahu, L. K., Kondo, Y., Takegawa, N., Han, S., Jung, J. S., Kim, Y. J., Fan, S., Sugimoto,
1048 N., Shammaa, M. H., Zhang, Y. H., and Zhao, Y.: Temporal variations of black carbon in
1049 Guangzhou, China, in summer 2006, *Atmos. Chem. Phys.*, 10, 6471-6485, doi: 10.5194/acp-10-6471-
1050 2010, 2010.

1051 WHO: Air quality guidelines: global update 2005: particulate matter, ozone, nitrogen dioxide, and sulfur
1052 dioxide, World Health Organization, 2006.

1053 Wiedinmyer, C., Akagi, S. K., Yokelson, R. J., Emmons, L. K., Al-Saadi, J. A., Orlando, J. J., and Soja,
1054 A. J.: The Fire INventory from NCAR (FINN): a high resolution global model to estimate the
1055 emissions from open burning, *Geosci. Model Dev.*, 4, 625-641, doi: 10.5194/gmd-4-625-2011, 2011.

1056 Zhou, X., Gao, J., Wang, T., Wu, W., and Wang, W.: Measurement of black carbon aerosols near two
1057 Chinese megacities and the implications for improving emission inventories, *Atmospheric*
1058 *Environment*, 43, 3918-3924, 10.1016/j.atmosenv.2009.04.062, 2009.

1059 **Table 1.** Summary of instruments deployed during monitoring in Lumbini

Instrument (Model)	Manufacturer	Parameters	Inlet/sensor height (above ground)	Sampling interval	Sampled period
Environmental Dust monitor (EDM 164)	GRIMM Aerosol Technik, Germany	PM ₁ , PM _{2.5} , PM ₁₀	5 m	5 min	01/04-15/06
Aethalometer (AE42)	Magee Scientific, USA	Aerosol light absorption at seven wavelengths, and BC concentration	3 m	5 min	01/04-05/06
CO analyzer (48i)	Thermo Scientific, USA	CO concentration	3 m	1 min	01/04-15/06
O ₃ analyzer (49i)	Thermo Scientific, USA	O ₃ concentration	3 m	1 min	01/04-15/06
Automatic Weather Station (AWS)	Campbell Scientific, UK	T, RH, WS, WD, Global Radiation, Precipitation	12 m	1 min	01/04-15/06

1060

1061

1062 **Table 2.** Comparison of PM_{2.5}, BC, CO and O₃ concentrations at Lumbini with those at other sites in South Asia

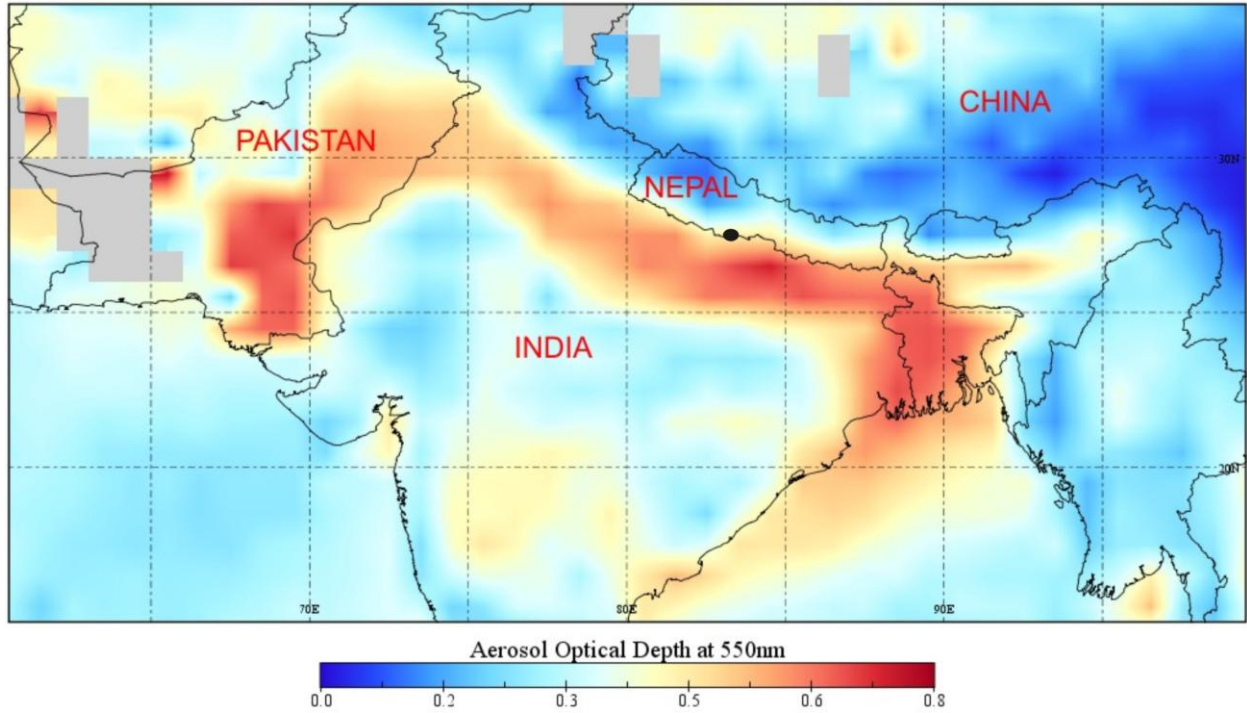
Sites	Characteristics	Measurement period	PM _{2.5} (µg m ⁻³)	BC (µg/m ³)	CO (ppbv)	O ₃ (ppbv)	References
Lumbini, Nepal	Semi-urban	Pre-monsoon, 2013	53.1±35.1	4.9±3.8	344.1±160.3	46.6±20.3	This study
Kathmandu, Nepal	Urban	Pre-monsoon, 2013	-	14.5±10	-	38.0±25.6	(Putero et al., 2015b)
Mt. Everest, Nepal	Remote	Pre-monsoon	-	0.4±0.4	-	61.3±7.7	(Marinoni et al., 2013)
Delhi, India	Urban	Pre-monsoon (night-time)	82.3±50.5	7.70±7.25	1800±890	-	(Bisht et al., 2015)
Kanpur, India	Urban	June 2009-May 2013, April-June	-	2.1±0.9	721±403	27.9±17.8	(Gaur et al., 2014) (Ram et al., 2010)
Mohali, India	Semi-urban	May, 2012	104±80.3	-	566.7±239.2	57.8±25.4	(Sinha et al., 2014)
Mt. Abu, India	Remote	Jan 1993-Dec 2000, pre-monsoon	-	0.7±0.14	131±36	39.9±10.8	(Naja et al., 2003) (Das and Jayaraman, 2011)

1063 **Table 3.** Inter-comparison of observed and model simulated hourly average concentrations of air
1064 pollutants during the measurement campaign period. Unit: BC and PM in $\mu\text{g}/\text{m}^3$ and CO in ppbv.

Pollutants	Observed (mean and range)	Modeled (mean and range)	Ratio of mean (observed/modeled)
BC	4.9 (0.3-29.9)	1.8 (0.4-3.7)	2.7
PM₁	36.6 (3.6-197.6)	12.3 (0.9-41.7)	3
PM_{2.5}	53.1 (6.1-272.2)	17.3 (1.9-48.3)	3
PM₁₀	128.8 (10.5-604.0)	25.4 (2.1-68.8)	5
CO	344.1(124.9-1429.7)	255.7 (72.2-613.1)	1.4

1065

1066



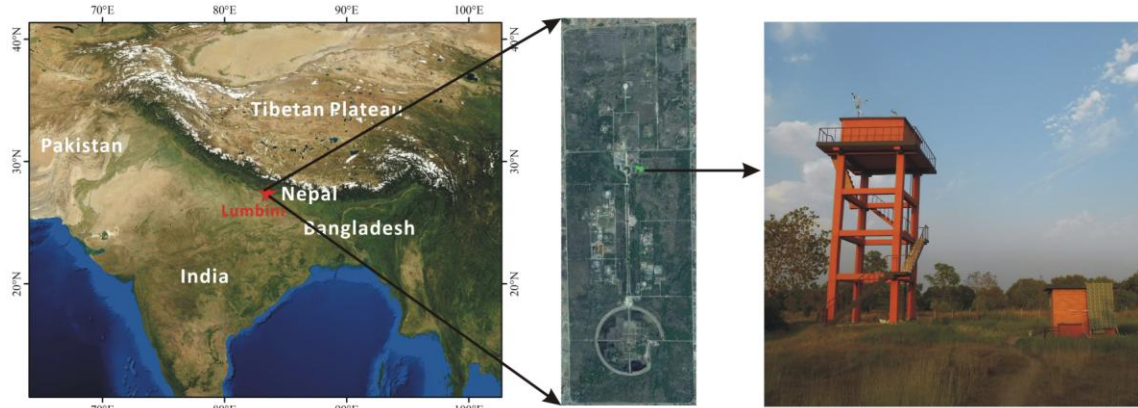
1068

1069 **Figure 1.** Aerosol optical depth in South Asia acquired with the MODIS instrument aboard
1070 TERRA satellite averaged over the winter and pre-monsoon season (December 2012-June 2013).

1071 High aerosol loading can be seen over the entire Indo-Gangetic Plains (IGP). An aerosol hotspot
1072 south of Lumbini (small black mark nearby the border of Nepal with India) is clearly visible.

1073 Light grey color used in the figure represents the absence of data.

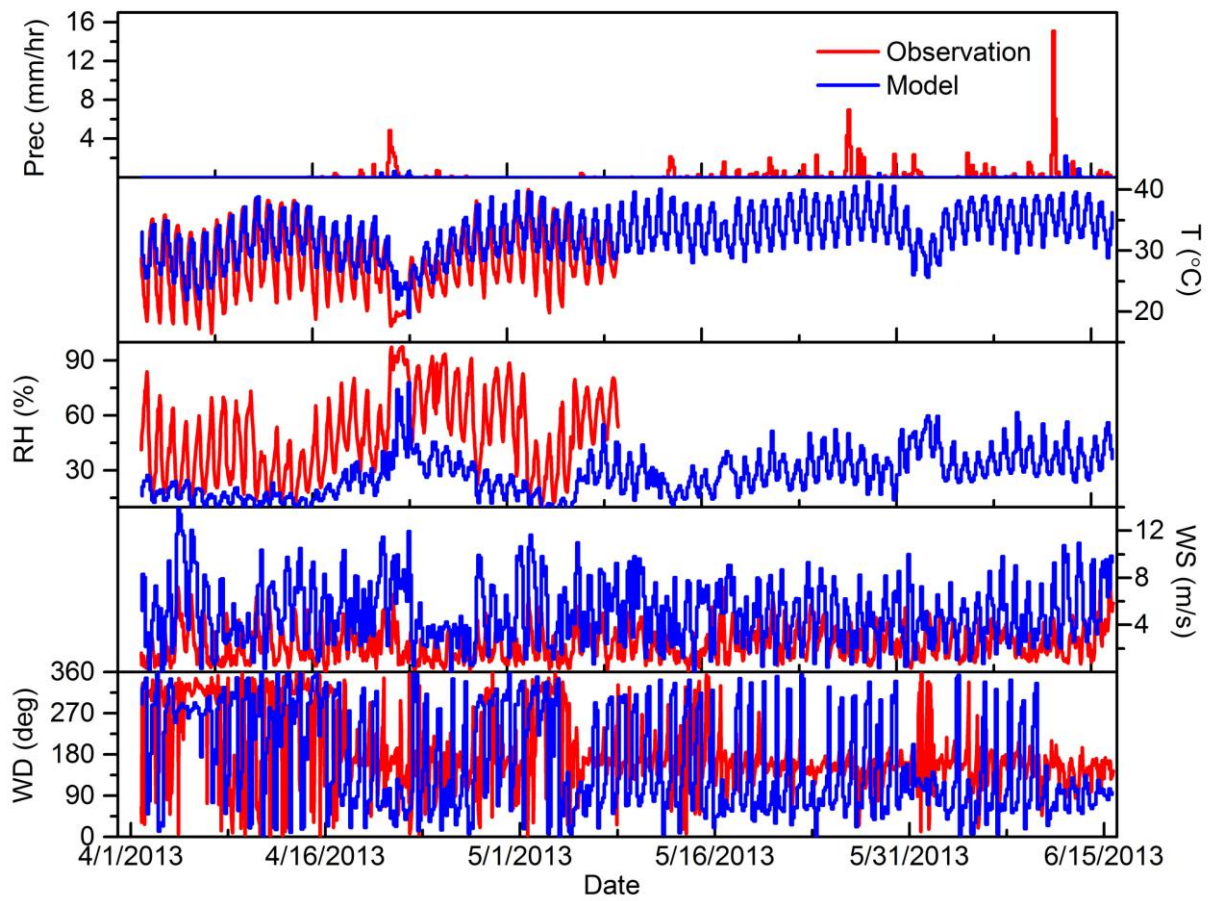
1074



1075

1076 **Figure 2.** Location of sampling site in Lumbini in southern Nepal (left panel). The middle panel
1077 shows the Kenzo Tange Master Plan Area of Lumbini while the right panel shows the sampling
1078 tower in the Lumbini Master Plan Area.

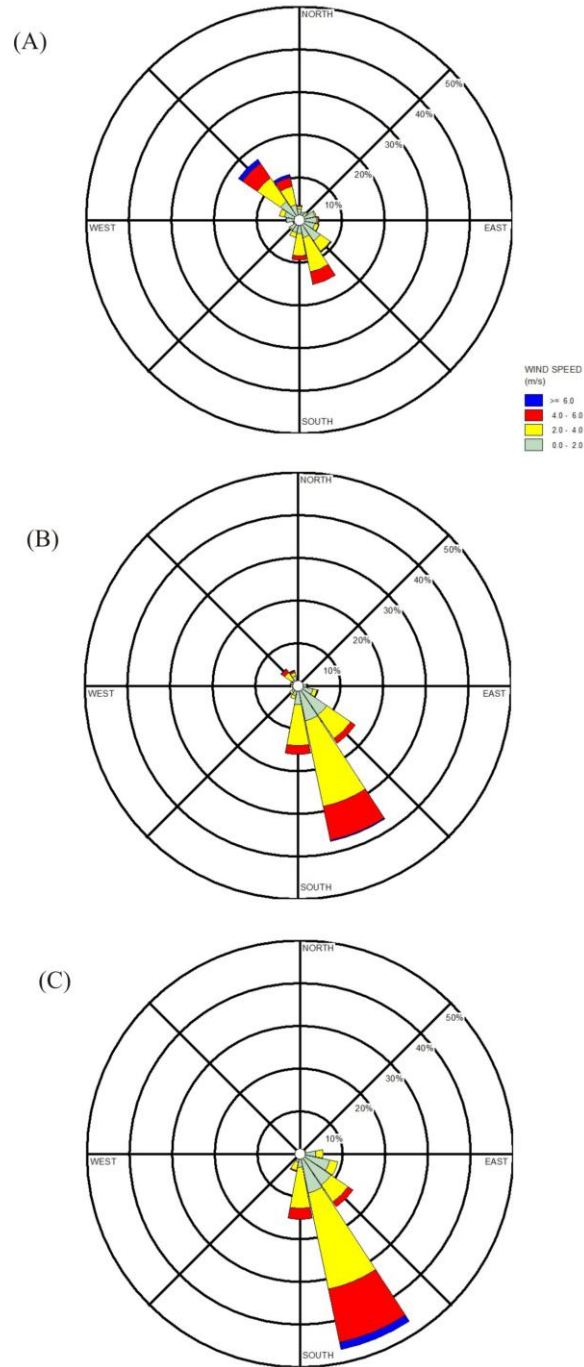
1079



1080

1081 **Figure 3.** Time series of hourly average observed (red line) and model estimated (blue line)
 1082 meteorological parameters at Lumbini, Nepal for the entire sampling period from 1 April to 15
 1083 June 2013.

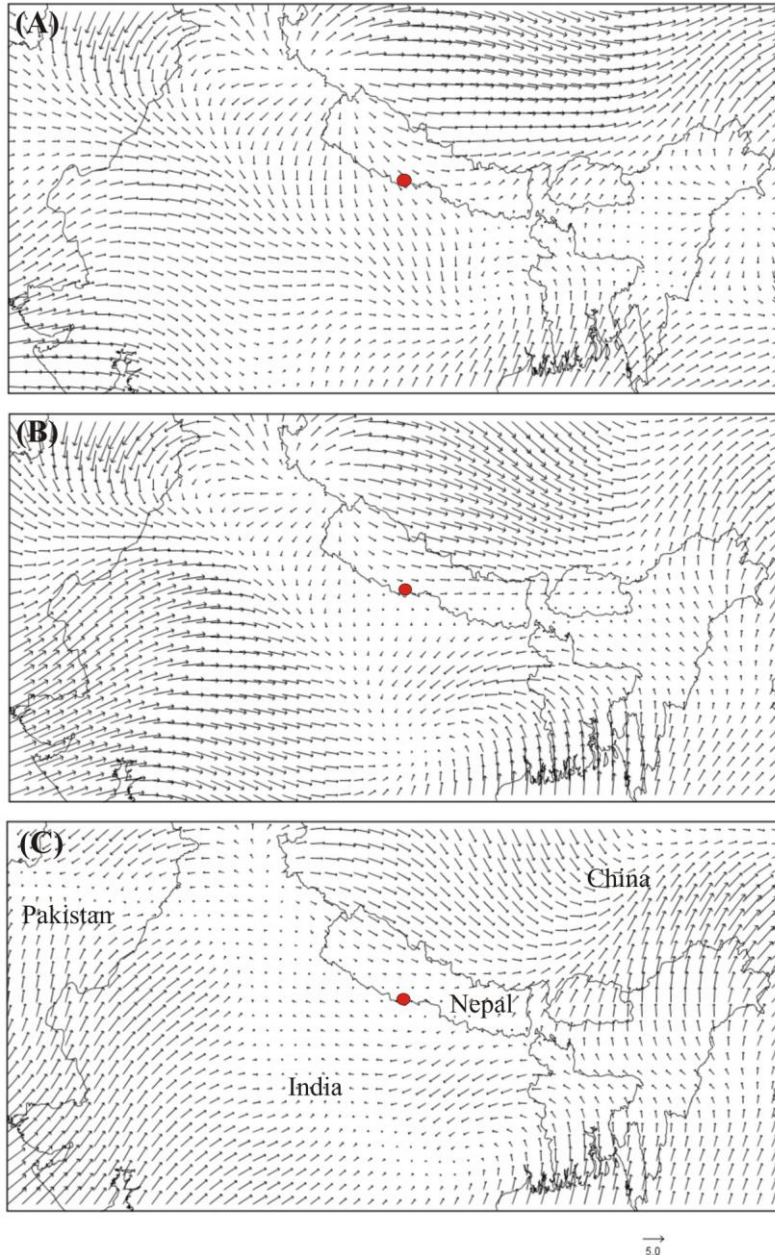
1084



1085

1086 **Figure 4.** Wind rose of wind speed and wind direction observed at Lumbini during the month of

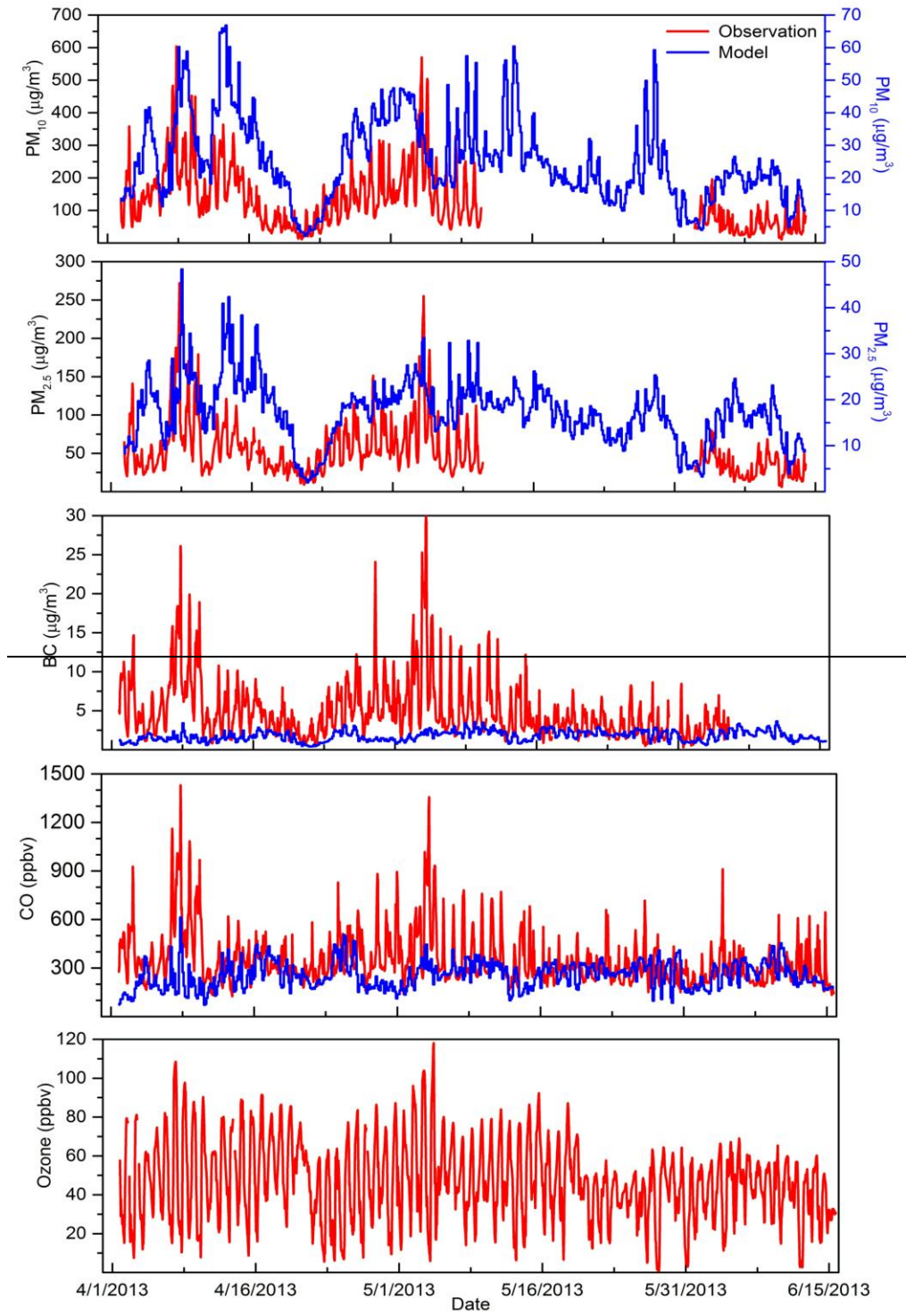
1087 (A) April, (B) May, and (C) (1st-15th) June 2013.



1088

1089 **Figure 5.** Monthly synoptic surface winds for the month of (A) April, (B) May and (C) June
 1090 2013, based on NCEP/NCAR reanalysis data. Orientations of arrows in the figures refer to wind
 1091 direction whereas the length of arrows represents the magnitude of wind speed (m/s). Red dot in
 1092 the map represents the location of Lumbini.

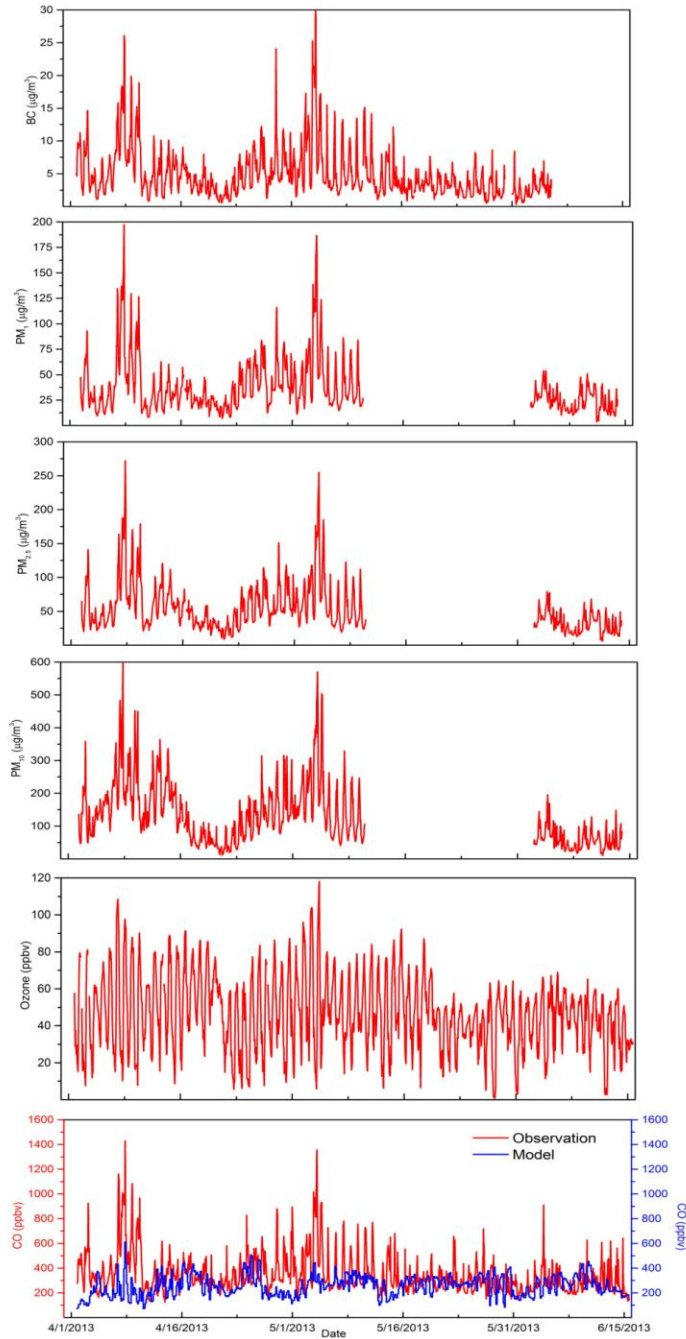
1093



1094

1095

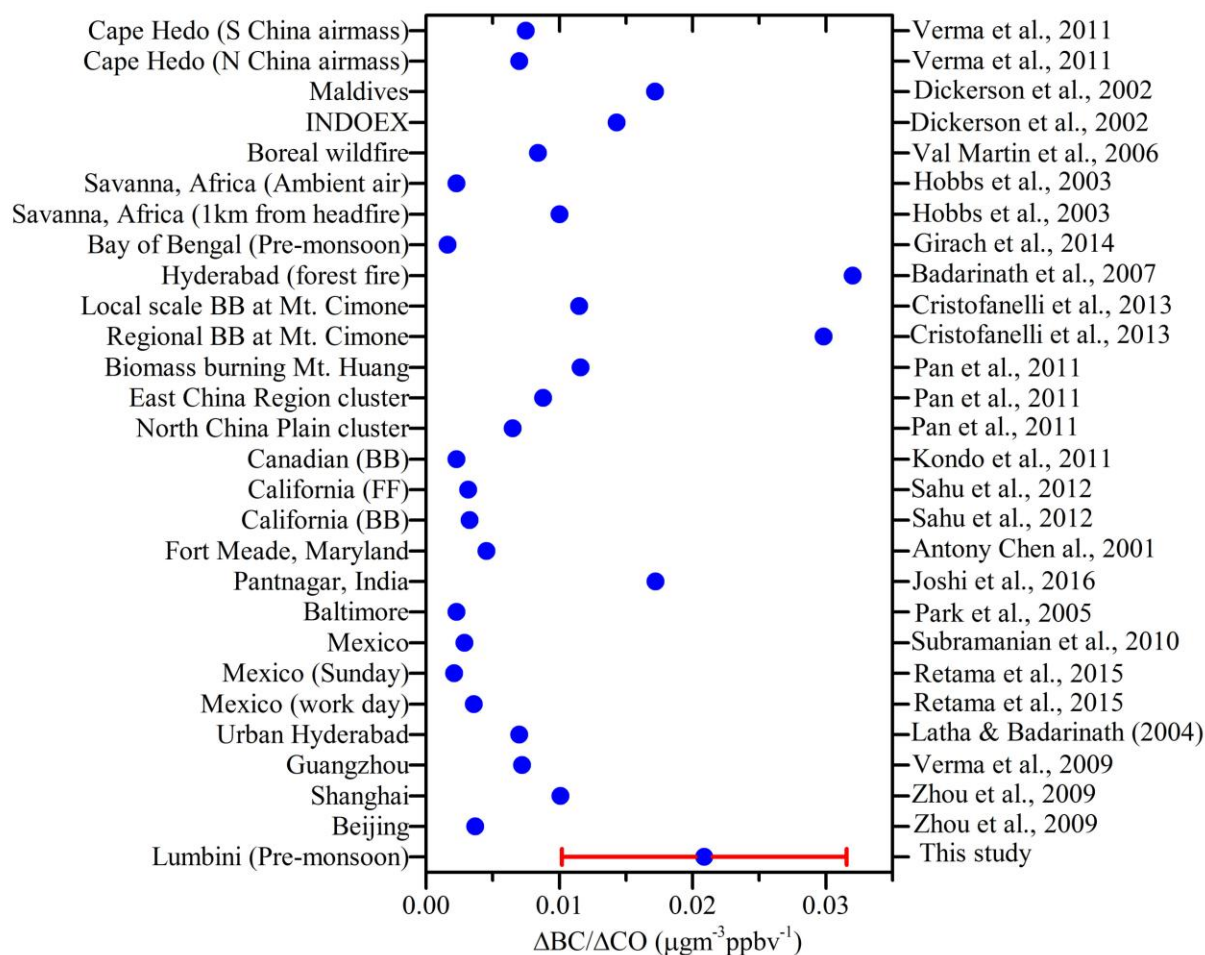
1096



1097

1098 **Figure 6.** Time series of the observed (red line) and model estimated (blue line) hourly average
 1099 concentrations of BC, PM₁, PM_{2.5}, PM₁₀, O₃ and CO at Lumbini, Nepal for the entire sampling
 1100 period from 1 April to 15 June 2013.

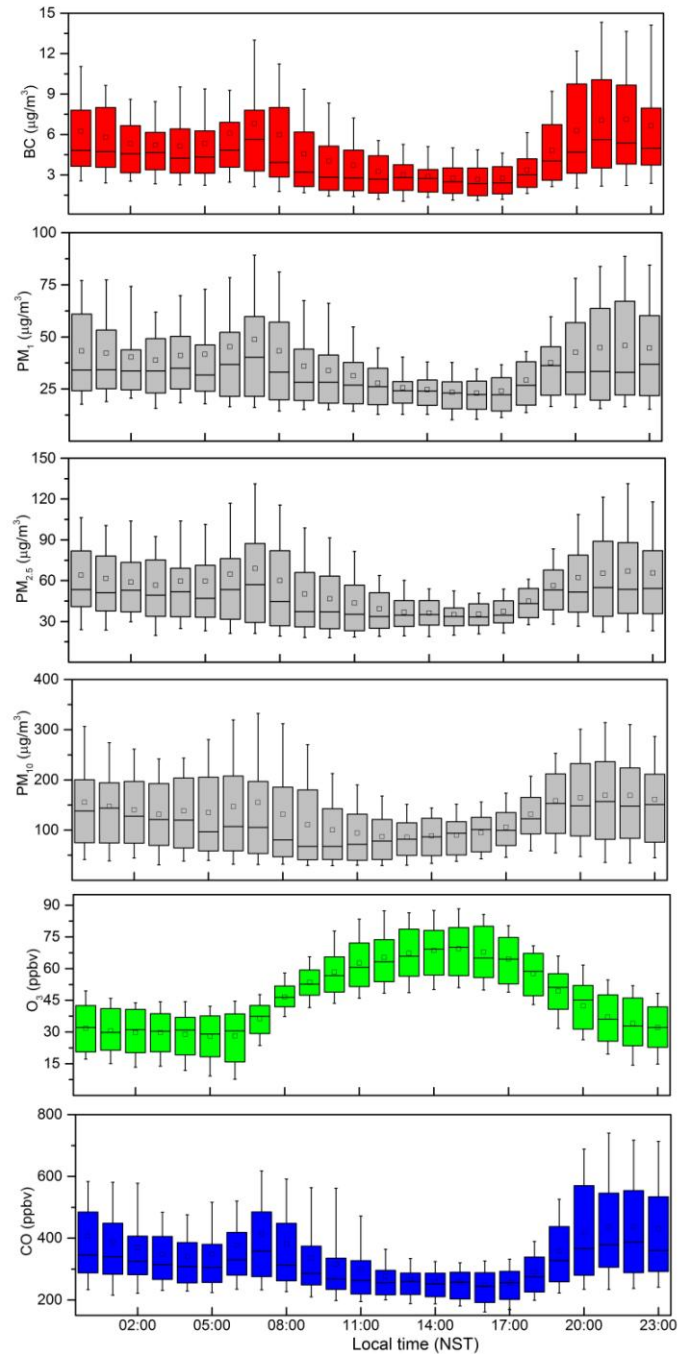
1101



1102

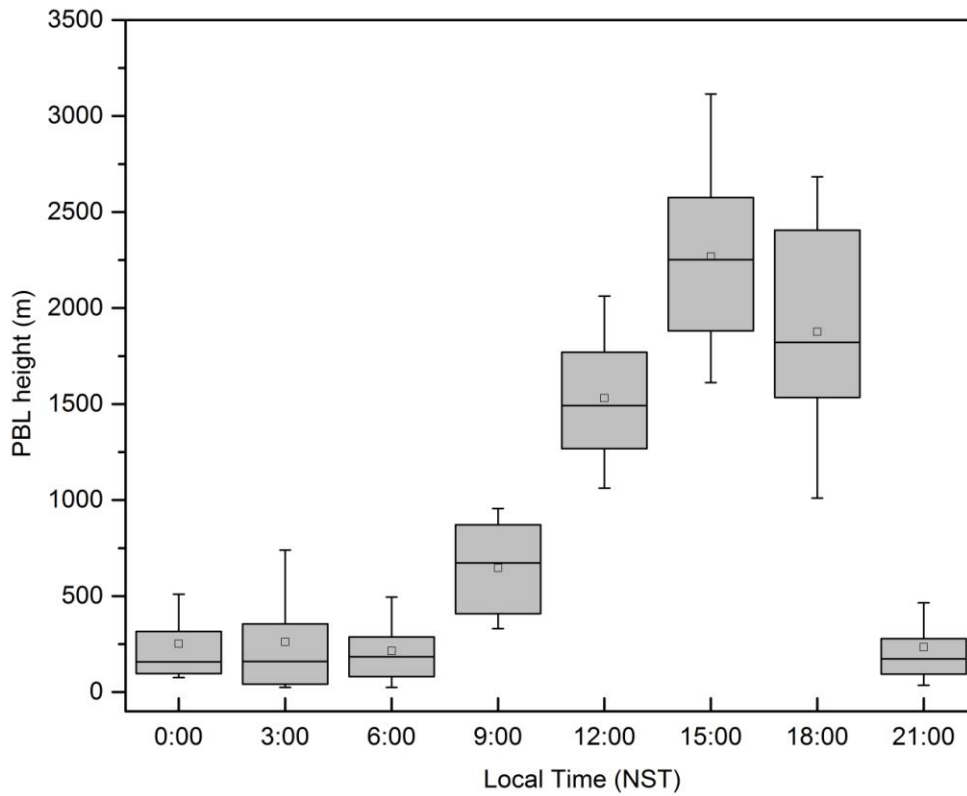
1103 Figure 7: Comparison of BC concentrations to CO concentrations ($\Delta BC/\Delta CO$) ratios obtained
 1104 for Lumbini with other sites. The red horizontal bar represents standard deviation.

1105



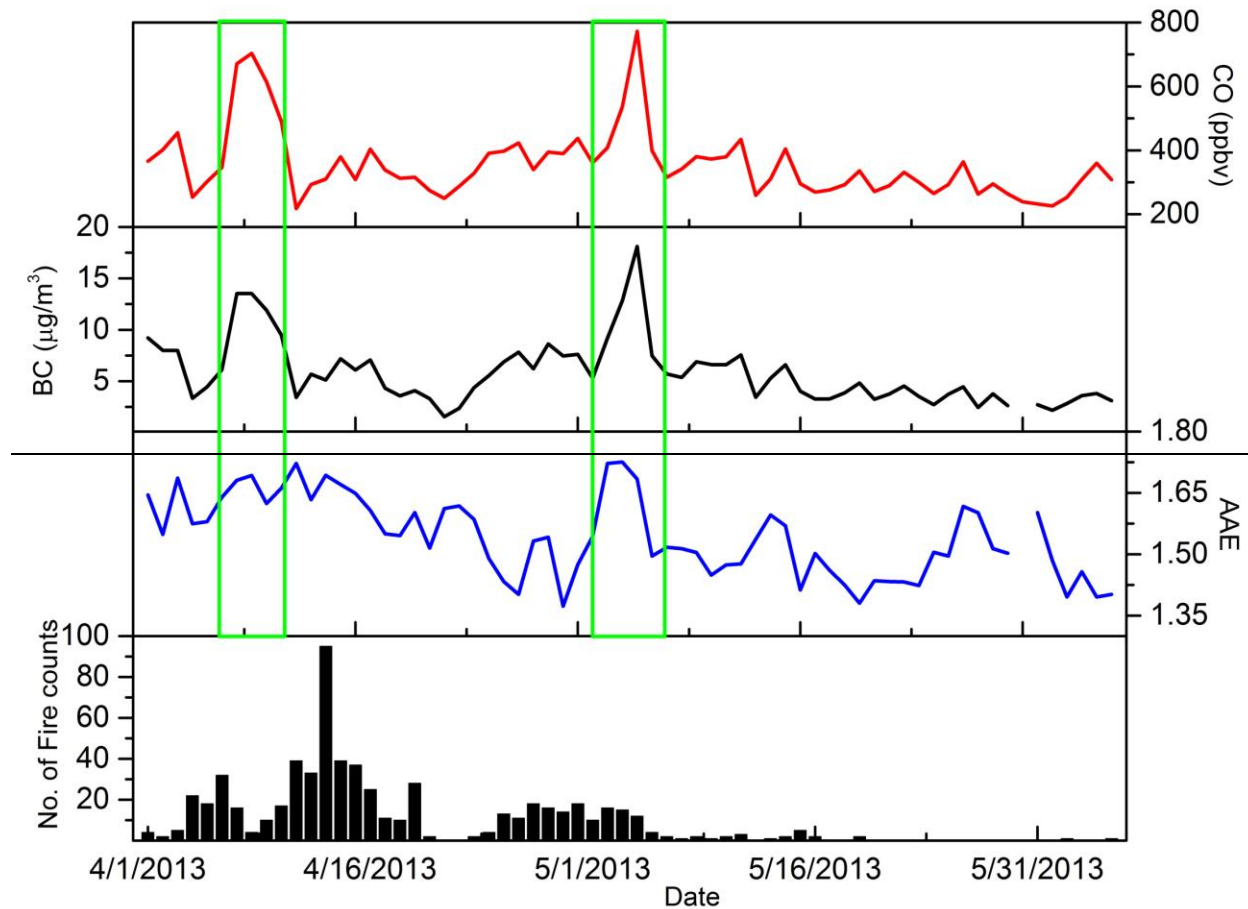
1106

1107 **Figure 8.** Diurnal variations of hourly average ambient concentrations of PM_{10} , BC , CO and O_3
 1108 BC , PM_1 , $PM_{2.5}$, PM_{10} , O_3 and CO at Lumbini during the monitoring period (1 April -15 June
 1109 2013). In each box, lower and upper boundary of the box represents 25th and 75th percentile
 1110 respectively, top and bottom of the whisker represents 90th and 10th percentile respectively, the
 1111 mid-line represents median, and the square mark represents the mean for each hour.



1112

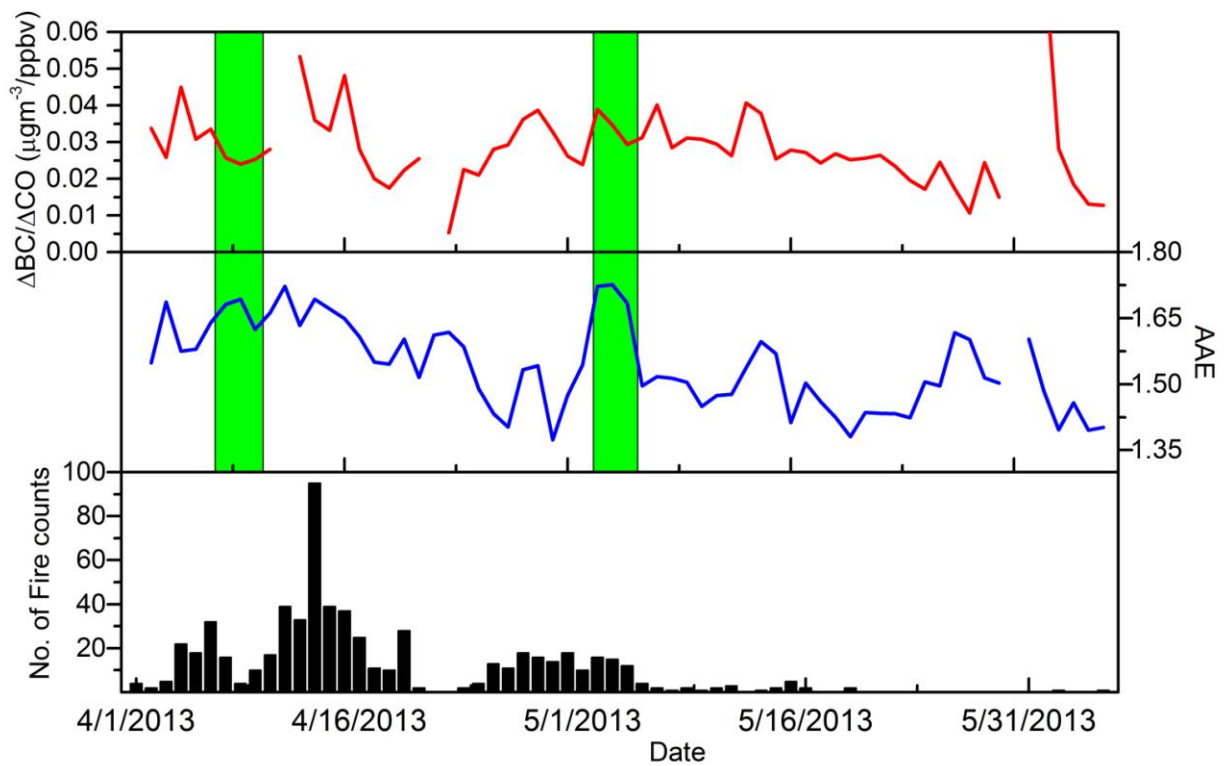
1113 **Figure 9.** Diurnal variation of the planetary boundary layer (PBL) height at Lumbini obtained
 1114 for every three hours of each day from the WRF-STEM model for the sampling period. The
 1115 square mark in each box represents the mean PBL height, bottom and top of the box represents
 1116 25th and 75th percentile, top and bottom of the whisker represents 90th and 10th percentile
 1117 respectively.



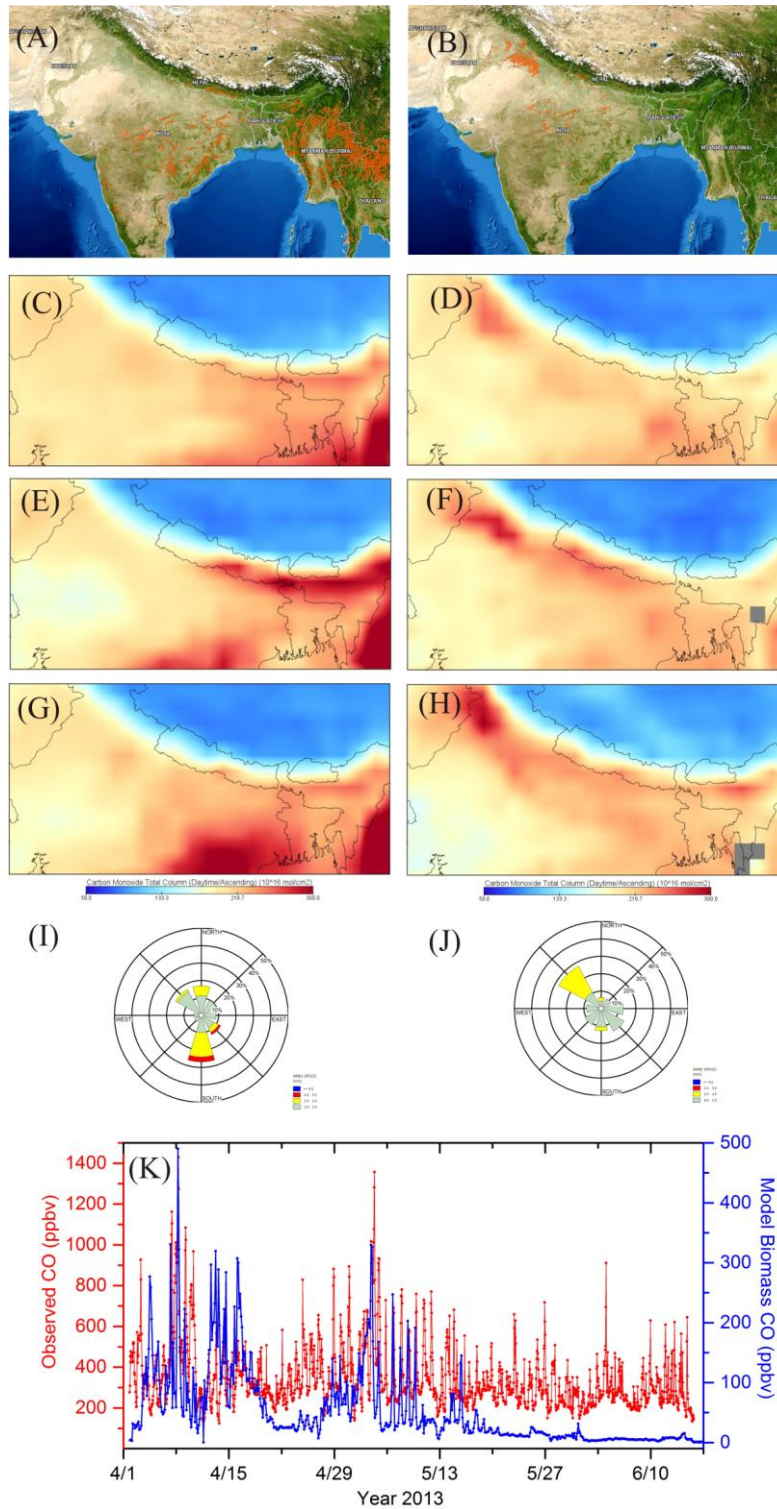
1118

1119 **Figure 9.** Time series of daily average CO, BC concentration, absorption Ångstrom exponent
 1120 (AAE), along with fire counts acquired with the MODIS instrument onboard TERRA satellite for
 1121 a 200x200 km grid centered at Lumbini. Two rectangular green boxes represent two episodes
 1122 with high peaks in CO and BC concentrations.

1123



1124
 1125 Figure 10. Time series of daily average $\Delta BC/\Delta CO$ ratio, absorption Ångstrom exponent (AAE),
 1126 along with fire counts acquired with the MODIS instrument onboard TERRA satellite for a
 1127 200×200 km grid centered at Lumbini. Two rectangular green boxes represent time of two
 1128 episodes with high peaks in CO and BC concentrations as shown in earlier figures.
 1129

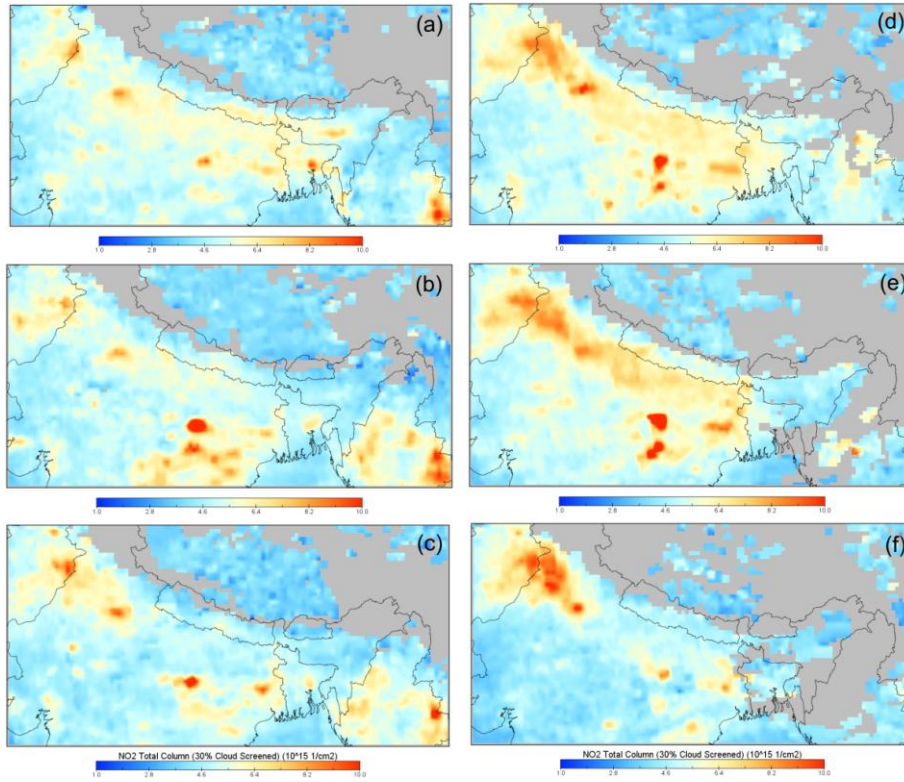


1130

1131 **Figure 11.** Active fire hotspots in the region acquired with the MODIS instrument on TERRA
 1132 satellite during (A) Event-I (7-9 April) and (B) Event-II (3-4 May). CO emissions, acquired with
 1133 AIRS satellite, in the region 2 days before (3-5 April), during (7-9 April) and 2 days after (10-12

1134 April) the Event-I are shown in panels (C), (E) and (G), respectively while panels (D), (F) and
1135 (H) show CO emissions 2 days before (1-2 May), during (3-4 May) and 2 days after (5-6 May)
1136 the Event-II. Panels (I) and (J) represent the average wind rose plot of observed wind direction
1137 and wind speed during Event I and II, respectively. (K) Observed CO versus Model open
1138 burning CO illustrating contribution of forest fires during peak CO loading.

1139

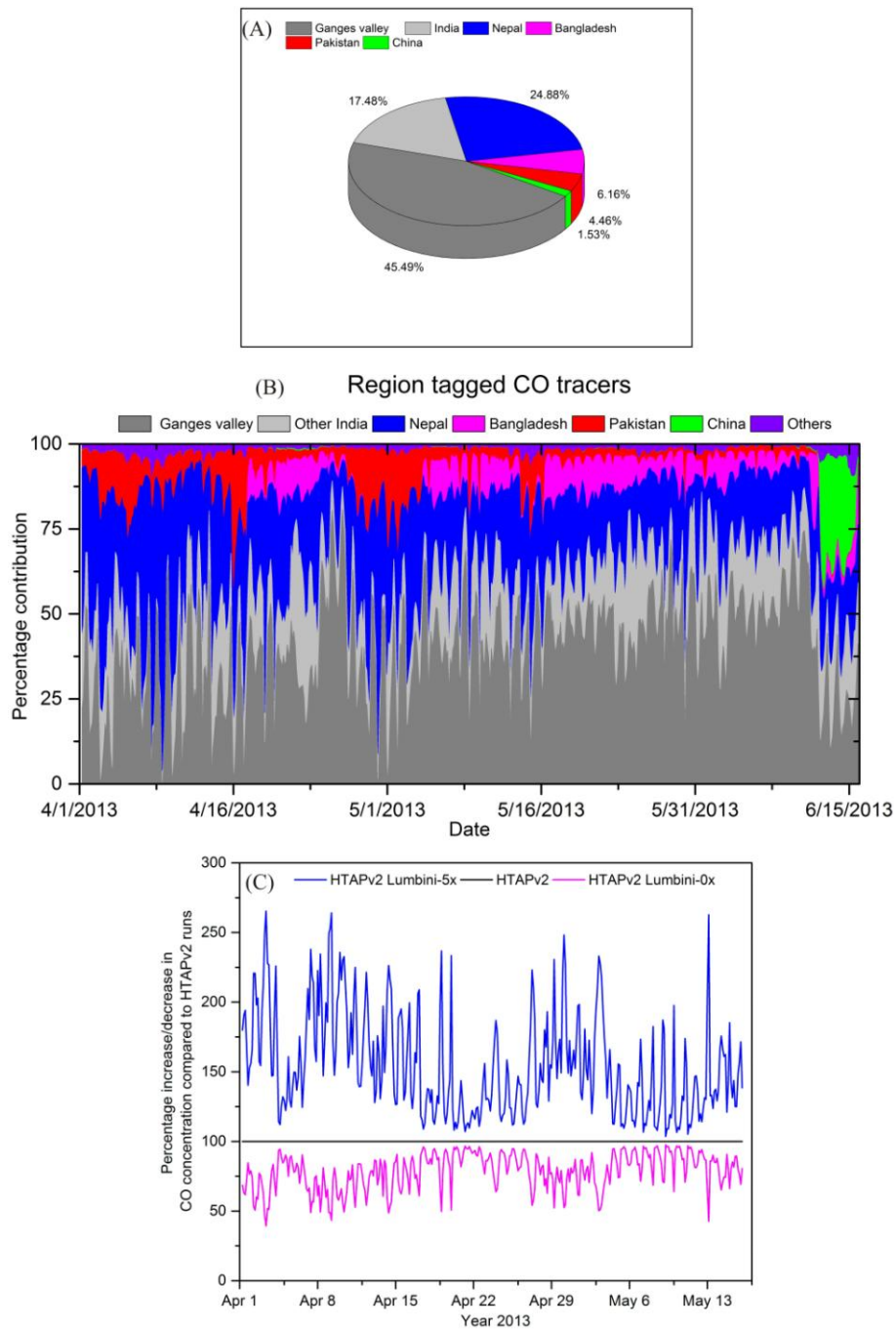


1140

1141 **Figure 12.** NO₂ total column obtained with OMI satellite over the region (a) before, (b) during,
 1142 and (c) after the Event- I. The panels (d), (e), (f) show NO₂ total column before, during and after
 1143 the Event- II.

1144

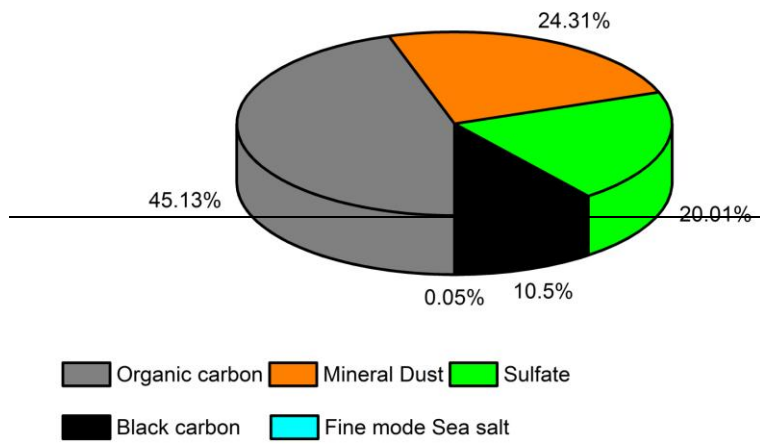
1145



1146

1147 **Figure 13.** (A) WRF-STEM model estimated contributions of various source regions to average
 1148 CO concentration in Lumbini for the sampling period, (B) time series of region tagged CO tracer
 1149 during the whole measurement period using HTAP emission inventory and (C) Figure showing
 1150 percentage increase/decrease in CO concentration with different emissions scenario.

1151

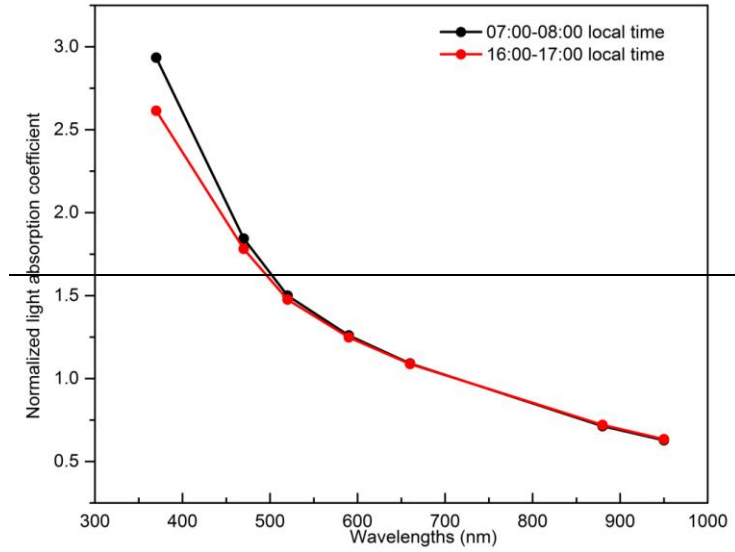


1152

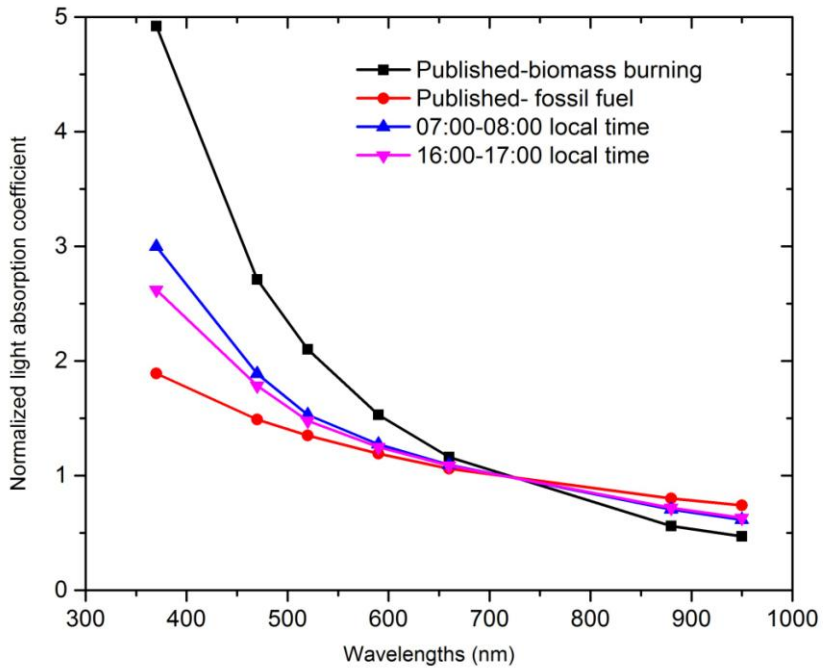
1153 **Figure 13.** WRF-STEM model estimated PM_{2.5} chemical composition at Lumbini for pre-
 1154 monsoon season 2013

1155

1156

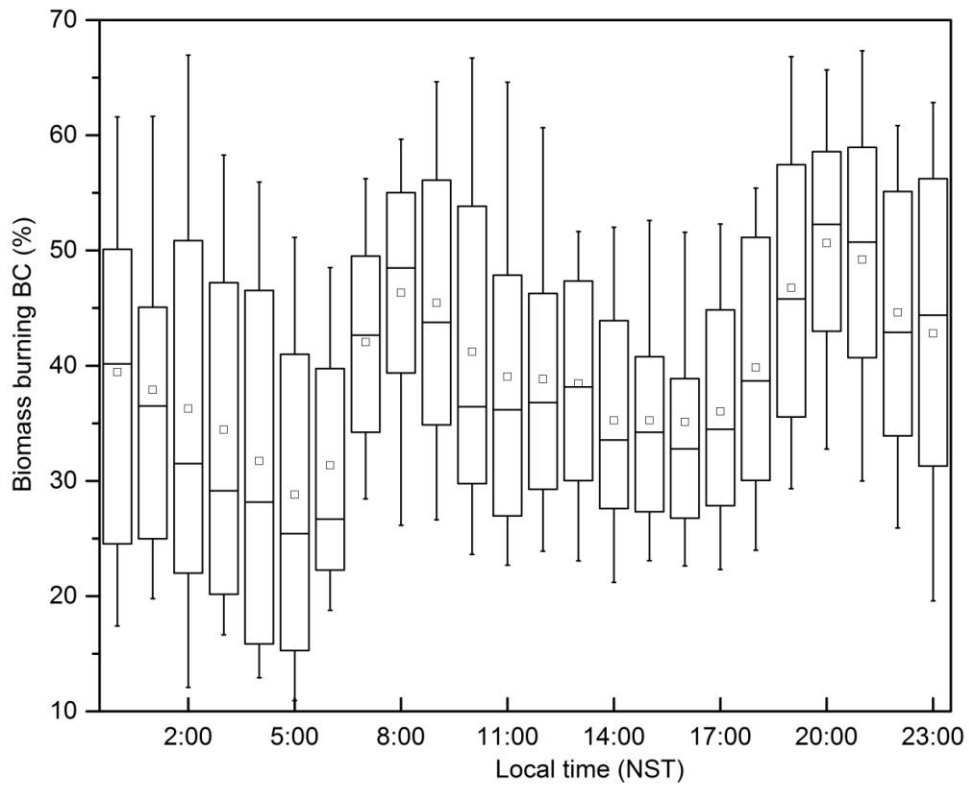


1157



1158 **Figure 14.** Comparison of normalized spectral light absorption coefficients obtained during the
1159 prime cooking (07:00-08:00 local time) and non cooking time (16:00-17:00 LT) at Lumbini with
1160 published data from Kirchstetter et al. (2004).

1161



1162

1163 **Figure 15.** Diurnal variation of the fractional contribution of biomass burning to ambient BC
 1164 concentration at Lumbini for the measurement period. In each box, lower and upper boundary of
 1165 the box represent 25th and 75th percentile, respectively, top and bottom of the whisker represents
 1166 90th and 10th percentile, respectively. The mid-line in each box represents median while the
 1167 square mark represents the mean for each hour.

1168

1169

1170

1171

1172

1173